Acquired resistance to CDK4/6 inhibition is associated with dysregulation of multiple pathways including cyclin D-CDK4/6-RB, EGFR/HER, AKT/mTOR and IFN signaling

Melanie Spears (melaniespears1@gmail.com)
Ontario Institute for Cancer Research https://orcid.org/0000-0002-1535-4675
Lauren Bathurst
Ontario Institute for Cancer Research
Linda Liao
Ontario Institute for Cancer Research
Megan Hopkins
Ontario Institute for Cancer Research
Cheryl Crozier
Ontario Institute for Cancer Research
Quang Trinh
Ontario Institute for Cancer Research
Emanuel Petricoin III
George Mason University
Jane Bayani
Ontario Institute for Cancer Research
John Bartlett
Ontario Institute for Cancer Research

Article

Keywords:

Posted Date: January 17th, 2024

DOI: https://doi.org/10.21203/rs.3.rs-3782509/v1

Additional Declarations: There is a conflict of interest EFP reports leadership, stock/ownership, consulting/advisory and travel funds from Perthera and Ceres Nanosciences; stock and consulting/advisory for Theralink Technologies, Inc., Perthera, Inc., and Ceres Nanosciences Inc.; support from Deciphera Pharmaceuticals, Springwork Therapeutics, Mirati Therapeutics, GlaxoSmithKline, Abbvie, Symphogen, and Genentech; patents/royalties from NIH, and is co-inventor of RPPA technology and issued and licensed patents for mTOR response predictors. JB receives grant research funds from Thermo Fisher Scientific; and holds a patent “95-Gene Signature of Residual Risk Following Endocrine Treatment in Early Breast Cancer”. JMSB reports Scientific Advisory Board participation with MedcomXchange Communications Inc; honoraria from bioTheranostics and MedcomXchange Communications Inc; consultancy/advisory for Insight Genetics, BioNTech AG, bioTheranostics, RNA Diagnostics, Pfizer, oncoXchange, Herbert Smith French Solicitors, OncoCyte Corporation, Ontario Institute for Cancer Research, AstraZeneca, Cerca Biotech and Tempus; research funding from NanoString Technologies, Stratifyer GmbH, Genoptix, Thermo Fisher Scientific, Agendia, Biotheranostics, Inc. and Exact Sciences; travel expenses from bioTheranostics; and holds three granted patents: “95-Gene Signature of Residual Risk Following Endocrine Treatment in Early Breast Cancer”, “CIN4 predicts benefit from anthracycline”, “Targeting the Histone Pathway to Detect and Overcome Anthracycline Resistance”, and three additional pending patents “Systems, Devices and Methods for Constructing and Using a Biomarker”, “Immune Gene Signature Predicts Anthracycline Benefit”, and “A Molecular Classifier for Personalized Risk Stratification for Patients with Prostate Cancer”. MS holds two granted patents: “Targeting the Histone Pathway to Detect and Overcome Anthracycline Resistance” and “Methods and Devices for Predicting Anthracycline Treatment Efficacy”.

Acquired resistance to CDK4/6 inhibition is associated with dysregulation of multiple pathways including cyclin D-CDK4/6-RB, EGFR/HER, AKT/mTOR and IFN signaling

Authors:
Lauren Bathurst[1,2], Linda Liao[2], Megan Hopkins[2], Cheryl Crozier[2], Quang Trinh[2], Emanuel F Petricoin[3], Jane Bayani[1,2], John MS Bartlett[4], Melanie Spears[1,2]

Affiliations:
1. Department of Laboratory Medicine and Pathobiology, University of Toronto, Toronto, ON, Canada.
2. Diagnostic Development, Ontario Institute for Cancer Research, Toronto, ON, Canada.
3. Center for Applied Proteomics and Molecular Medicine, George Mason University, Manassas, VA, USA.
4. University of Edinburgh, Edinburgh, Scotland, UK.

Author Contributions:
L.B., J.M.S.B. and M.S. conceived and designed the study. L.B., L.L., and M.S. developed the methodology. L.B. and L.L. performed the laboratory experiments. M.H. and C.C. performed Oncomine sequencing. Q.T. processed Oncomine mutation data. J.B. provided insights into the project. E.F.M performed and analyzed RPPA. L.B. and M.S. analyzed and interpreted the data. All authors have read and approved the final manuscript.

Acknowledgements:
This study was conducted with the support of the Ontario Institute for Cancer Research through funding provided by the Government of Ontario. The views expressed in the publication are the views of the authors and do not necessarily reflect those of the Government of Ontario.

Competing Interests:
EFP reports leadership, stock/ownership, consulting/advisory and travel funds from Perthera and Ceres Nanosciences; stock and consulting/advisory for Theralink Technologies, Inc., Perthera, Inc., and Ceres Nanosciences Inc.; support from Deciphera Pharmaceuticals, Springwork Therapeutics, Mirati Therapeutics, GlaxoSmithKline, Abbvie, Symphogen, and Genentech; patents/royalties from NIH, and is co-inventor of RPPA technology and issued and licensed patents for mTOR response predictors. JB receives grant research funds from Thermo Fisher Scientific; and holds a patent “95-Gene Signature of Residual Risk Following Endocrine Treatment in Early Breast Cancer”. JMSB reports Scientific Advisory Board participation with MedcomXchange Communications Inc; honoraria from bioTheranostics and MedcomXchange Communications Inc; consultancy/advisory for Insight Genetics, BioNTech AG, bioTheranostics, RNA Diagnostics, Pfizer, oncoXchange, Herbert Smith French Solicitors, OncoCyte Corporation, Ontario Institute for Cancer Research, AstraZeneca, Cerca Biotech and Tempus; research funding from NanoString Technologies, Stratifyer GmbH, Genoptix, Thermo Fisher Scientific, Agendia, Biotheranostics, Inc. and Exact Sciences; travel expenses from bioTheranostics; and holds three granted patents: “95-Gene Signature of Residual Risk Following Endocrine Treatment in Early Breast Cancer”, “CIN4 predicts benefit from anthracycline”, “Targeting the Histone Pathway to Detect and Overcome Anthracycline Resistance”, and three additional pending patents “Systems, Devices and Methods for Constructing and Using a Biomarker”, “Immune Gene Signature Predicts Anthracycline Benefit”, and “A

Molecular Classifier for Personalized Risk Stratification for Patients with Prostate Cancer". MS holds two granted patents: "Targeting the Histone Pathway to Detect and Overcome Anthracycline Resistance" and "Methods and Devices for Predicting Anthracycline Treatment Efficacy".

Code Availability:

All bioinformatic analyses were done using the R Statistical programming language (v.4.0.4). The specific packages, parameters, and versions used are outlined in their respective sections found in Methods. The code used in this study, including pipelines for filtering, processing, and analysis, is available upon reasonable request.

Running Head:

CDK4/6i resistance in early breast cancer

Abstract

While the use of CDK4/6 inhibitors has significantly improved outcomes for patients with ER+/HER2- tumours, understanding the mechanisms responsible for resistance is essential to identify predictive biomarkers and alternative treatment options after tumour progression. To this end, we developed *in-vitro* models of acquired resistance to palbociclib and abemaciclib using MCF7 and T47D cell lines. Genomic, transcriptomic, and proteomic analyses were used to identify potential actionable molecular alterations in these models. Results show that acquired resistance was associated with dysregulation of multiple signaling pathways, including cyclin D-CDK4/6-RB, EGFR/HER and AKT/mTORC1. Strikingly, acquired resistance across all cell lines was also associated with an upregulated interferon (IFN) response. Expression of an IFN-based gene signature derived from these models was upregulated in breast cancer cell lines and early-stage tumours intrinsically resistant to CDK4/6i, and thus warrants further clinical evaluation as a predictive biomarker of resistance.

Introduction

Treatment with CDK4/6 inhibitors (CDK4/6i) palbociclib, ribociclib and abemaciclib in combination with endocrine therapy significantly improves progression-free survival (PFS) and overall survival (OS) in patients with advanced/metastatic ER+/HER2- breast cancer (BC)[1–9]. Recently, abemaciclib was also shown to significantly improve invasive disease-free survival (IDFS) in patients with high-risk early-stage disease[10,11]. However, many patients will experience disease progression due to intrinsic or acquired resistance. Preclinical and clinical studies have shown that resistance may arise through dysregulation of cell cycle components including loss of RB1[12–24], as well as amplification and/or overexpression of CDK6[19,25–27], cyclin E1[17,18,28], or AURKA[29]. Resistance has also been associated with hyperactivation of several signaling pathways, including FGFR[29–32], HER2[29,33], PI3K/AKT/mTOR[17,22–24,29,34,35], RAS/ERK[29,36] and most recently, interferon (IFN) signaling[37].

While the understanding of CDK4/6i sensitivity and resistance continues to evolve, there remains at present no biomarker to select patients for treatment with CDK4/6i other than ER+/HER2- status in either the early-stage or advanced/metastatic BC settings. Identification of predictive biomarkers, and patient subgroups most likely to benefit from treatment, is essential to further improve patient outcomes and spare those who are unlikely to benefit from unnecessary toxicities. Determination of the optimal treatment options after resistance develops, as well as therapeutic targets to enhance initial CDK4/6i efficacy, will also require a better understanding of the mechanisms responsible for resistance.

In this study, *in-vitro* models of acquired resistance to two CDK4/6i, palbociclib and abemaciclib, were developed and characterized by a series of -omics analyses. These data demonstrate that multiple pathways are dysregulated in resistant cell lines including, cyclin D-CDK4/6-RB, EGFR/HER, AKT/mTORC1, and IFN signaling. Notably, while other acquired molecular changes varied between cell lines, an IFN response was consistently upregulated in all models, providing further support that IFN signaling plays an important role in the development of resistance to CDK4/6i. An IFN-based gene signature was derived from these models and predicted intrinsic resistance to palbociclib *in-vitro* as well as *in-vivo* in patient tumours, representing a potential predictive biomarker of resistance for further evaluation.

Results

Resistant cells are cross resistant to other CDK4/6i and endocrine therapies

MCF7 and T47D resistant cell lines were generated by treatment with increasing concentrations of CDK4/6i palbociclib or abemaciclib over the course of 8-10 months. The resulting cell lines were designated palbociclib-resistant (PR) or abemaciclib-resistant (AR), respectively: one of each for MCF7 (MCF7-AR and MCF7-PR) and T47D (T47D-AR and T47D-PR). Dose-response curves were used to determine growth rate (GR) inhibition values. GR75 values are reported when inhibitors are unable to elicit a 50% growth rate inhibition (GR50) in parental lines. Resistant cells either did not reach GR75 or had GR75 values 24-180-fold higher than their parental counterparts (Fig. 1a). Cross resistance to other CDK4/6i was also observed in all four models (Fig. 1a). Treatment with 0.5μM or 1μM of CDK4/6i significantly increased the percentage of cells in G0/G1-phase in parental cell lines compared to resistant cell lines (88-89% vs 47-73% in G0/G1-phase, respectively) (Supplementary Fig. 1a). Flow cytometry-based cell cycle analysis uncovered an increase in 4n cells, as well as a gain of an 8n peak in T47D-AR cells, indicative of an acquired mitotic defect (Supplementary Fig. 1b). CDK4/6i resistance was also associated with loss of ER/PR mRNA and protein expression, as well as reduced response to endocrine therapies, tamoxifen and fulvestrant (GR75 values 2-5-fold higher than parental cells) (Fig. 1b-d). To assess stability of the CDK4/6i resistance phenotype, resistant cell lines were cultured in the absence of drug for 6 months. Dose-response curves showed that long-term drug removal did not restore CDK4/6i sensitivity to parental levels (Fig. 1e). Together these results confirm that CDK4/6i resistant cells are cross-resistant to other CDK4/6i as well as endocrine therapy[21,22,25,38].

Acquired genomic changes in cell cycle and EGFR/HER signaling pathways

Targeted sequencing was performed to identify genomic changes associated with CDK4/6i resistance. Resistant cell lines acquired between 2 to 5 additional genomic alterations (Fig. 2, Supplementary Table S1). Copy number changes included loss of *RB1* in all four resistant models. In addition, *RB1* mutations were acquired in three of four models. Other alterations included low-level gains of *EGFR* (1-4 copies) in both MCF7 derivatives, as well as acquired *BRAF* and *NF1* mutations in MCF7-PR and T47D-AR cell lines (Fig. 2, Supplementary Table S1). In concordance with *RB1* copy number loss, reduced *RB1* mRNA (2-50-fold) and protein expression was observed in all four resistant models (Fig. 3a, b). This prompted evaluation of additional CDKs and cyclins required for G0/G1-S-phase transition. Despite the absence of genomic amplification, *CCNE1* mRNA expression was significantly increased in T47D resistant models (1.5-3-fold) (Fig. 3a). Cyclin E protein expression was also elevated in all four resistant cell lines (Fig. 3b). *CDK6* mRNA expression was significantly increased in MCF7-AR cells (2-fold); greater increases were observed in both T47D resistant models (7.5-15-fold) (Fig. 3a). CDK6 protein was also elevated in these models (Fig. 3b).

In concordance with *EGFR* copy number gains, mRNA levels were significantly increased in both MCF7 resistant models (3.5-5.5-fold) as well as in T47D-PR cells (1.3-fold) (Fig. 3a). Total EGFR protein expression was also elevated in these models (Fig. 3c). In contrast, *EGFR* mRNA (1.7-fold) and protein expression was reduced in T47D-AR cells (Fig. 3a, c). This prompted evaluation of additional HER-family members. A reduction in *ERBB2* mRNA expression was evident in both T47D resistant models (1.7-2-fold), while *ERBB3* mRNA expression was also reduced in T47D-PR cells (1.7-fold) (Fig. 3a). Total expression as well as phosphorylation of EGFR, HER2 and HER3, were reduced in T47D-AR cells, suggesting a decrease in EGFR/HER signaling (Fig. 3c). In addition, total HER3 expression and phosphorylation was reduced in T47D-PR cells. In contrast, phosphorylation of EGFR was elevated in both MCF7 resistant models (Fig. 3c)

Transcriptomic and proteomic analyses uncover changes in AKT/mTOR and IFN signaling

Transcriptomic and proteomic analyses were performed to further investigate the molecular changes associated with acquired resistance. RNA-seq analyses demonstrated that resistant models underwent extensive transcriptomic changes to adapt to prolonged CDK4/6i exposure. A total of 1917-4471 and 1905-3590 genes were differentially expressed in MCF7 and T47D derivatives, respectively, compared to their parental cell lines (Fig. 4a). GSEA was performed to identify signaling pathways associated with acquired resistance. The most significantly altered gene sets were categorized by common biological processes: IFN response, chromosome maintenance/DNA repair, regulation of neurogenesis, axonogenesis, cell adhesion, eukaryotic translation, synapse organization and assembly, hallmark E2F targets, estrogen response, and nicotinate metabolism (FDR<0.001) (Fig. 4b, Supplementary Table S2, S3). Strikingly, genes relating to IFN response were significantly enriched in all four models. RT-qPCR was used to confirm significant upregulation of 7 representative IFN stimulated genes (ISGs). Expression of STAT1, IFI6, IFI44, IFIT1, MX1, OAS1, and OAS2 were 2-8 log2-fold higher in resistant cell lines relative to parental lines (Fig. 4c).

Finally, proteomic analysis performed by RPPA identified a total of 8 proteins as significantly differentially expressed in all four resistant models (Fig. 4d, Supplementary Table S4). In line with RNA-seq data, phosphorylation of STAT1 was significantly upregulated, consistent with activated IFN signaling. This was confirmed by western blot (Fig. 4e). Phosphorylated RB, STAT5 and HER3 were among downregulated proteins (Fig. 4d). A significant increase in p70S6K was observed in both T47D derivatives, while a significant reduction was observed in both MCF7s (Fig. 4d). These results suggested up and downregulation of mTORC1 signaling in these models, respectively. Upregulated p70S6K in T47D cells was confirmed by western blot (Fig. 4f). In summary, there was strong concordance between the results of genomic, transcriptomic, and proteomic analyses. Notably, while acquired resistance to CDK4/6i was associated with dysregulation of multiple signaling pathways including, cyclin D-CDK4/6-RB, EGFR/HER and AKT/mTORC1, dysregulation of IFN signaling was consistently observed across all models.

Therapeutic targeting of JAK-STAT signaling does not affect resistant cell proliferation

Canonical STAT1 activation occurs downstream of IFN receptor-associated Janus kinase (JAK)-1/2 kinases. To determine whether the IFN response upregulated in resistant models represents a targetable weakness, cell lines were screened with JAK1/2 inhibitors (JAK1/2i), ruxolitinib or tasocitinib. Treatment with JAK1/2i reduced STAT1 phosphorylation, demonstrating that these inhibitors effectively reached their targets (Fig. 5a). However, JAK1/2 inhibition had no effect on cell viability, nor did it re-sensitize resistant cells to CDK4/6 inhibition (Fig. 5b, c). In addition, JAK1/2i did not enhance the effects of CDK4/6i in parental cell lines (Fig. 5c). Together these results suggest that canonical JAK/STAT signaling is associated with acquired resistance to CDK4/6i *in-vitro* but does not appear to drive cell growth or proliferation.

Upregulated IFN signaling is associated with intrinsic resistance to CDK4/6i *in-vitro* and in patient tumours

While multiple acquired molecular alterations were uncovered through -omics analyses, IFN signaling was consistently upregulated in all resistant models and was therefore the focus of potential biomarker development. Transcriptomic data from resistant cell lines was used to derive an IFN-based gene signature associated with acquired resistance by selecting all genes significantly upregulated in all four models (IFN-sig). To determine whether the IFN-sig could predict intrinsic resistance to CDK4/6i, we

evaluated sensitivity to palbociclib in a panel of 15 ER+/HER2- BC cell lines (Fig. 6a). GR50 values ranged from 78nM to >5uM. Among these, MDAMB134, MDAMB175, 600MPE, and CAMA-1 were the most sensitive to palbociclib (GR50 78-306nM). Five cell lines did not reach GR50 (GR50 >5μM): BT483, HCC1428, KPL1, ZR75 and ZR75B. The four most sensitive cell lines were also among the most sensitive to ribociclib (GR50 116-929nM) and abemaciclib (GR50 21-177nM), highlighting mechanistic similarities between different CDK4/6i (Fig. 6a). Similarly, the most palbociclib resistant cell lines were also among the most resistant to ribociclib and abemaciclib (Fig. 6a). As previously reported[39], abemaciclib was the most potent of the three inhibitors, followed by palbociclib and then ribociclib. Publicly available RNA-seq data for these cell lines was profiled[40]. Importantly, genes from the IFN-sig were significantly enriched in palbociclib resistant cell lines compared to sensitive ones (Fig. 6b). Expression of the genes from the IFN-sig were also enriched in tumours resistant to neoadjuvant palbociclib plus anastrozole from the NeoPalAna trial[41] (Fig. 6c). These results provide further support that IFN signaling can predict resistance to CDK4/6i[37] and propose a novel IFN-based gene signature as a potential predictive biomarker for further clinical evaluation.

Discussion

We developed *in-vitro* models of acquired resistance to two different CDK4/6i, palbociclib and abemaciclib. Mechanisms responsible for resistance were diverse and included dysregulated cyclin D-CDK4/6-RB, EGFR/HER, AKT/mTOR and IFN signaling. Importantly, these pathways represent therapeutic opportunities to inhibit resistant cell growth and/or enhance the efficacy of CDK4/6i in parental cells. Intriguingly, an IFN response was consistently upregulated in all models, suggesting that IFN signaling plays an important role in CDK4/6i resistance.

IFN signaling can either promote or inhibit tumour growth depending on the strength and duration of exposure via direct effects on tumour cells and tumour-immune interactions[42]. Acute IFN exposure promotes anti-tumour activity by suppressing Tregs and stimulating tumour antigen presentation, and NK and cytotoxic T cell activity[43]. Historically, IFNs have also shown anti-tumour effects by inducing apoptosis and inhibiting cell cycle progression in BC[44]. In contrast, persistent IFN exposure promotes T-cell exhaustion and is associated with resistance to multiple therapy types including immunotherapy, chemotherapy, radiotherapy, and endocrine therapy[45–50]. More recently, De Angelis et al. showed that resistance to CDK4/6 inhibition was also associated with an IFN response *in-vitro*[37]. Clinically, ISG signatures were significantly enriched in tumours intrinsically resistant to neoadjuvant palbociclib or abemaciclib in combination with anastrozole (NeoPalAna, Neo-MONARCH)[37]. Subsequent analysis of two separate trials suggests that ISGs are also enriched in tumours resistant to neoadjuvant palbociclib plus letrozole (PALLET)[51,52], as well as palbociclib plus fulvestrant in metastatic disease after progression on endocrine therapy (PALOMA-3)[53]. Using independently derived models, our results provide further support that IFN signaling is associated with both *de novo* and acquired resistance to CDK4/6i *in-vitro*. Moreover, we derived an IFN-related gene signature predictive of intrinsic resistance to CDK4/6i in a panel of ER+/HER2- cell lines as well as *in-vivo* using patient tumours. If validated in additional clinical datasets, the IFN-sig could identify patients unlikely to respond to CDK4/6i, redirecting them towards alternative therapies.

These results highlight IFN signaling as a potential targetable weakness in CDK4/6i resistant cells. However, we also demonstrated that JAK1/2 inhibition had no effect on cell viability in resistant models, despite on-target reduction of pSTAT1. Moreover, JAK1/2 inhibition was unable to re-sensitize resistant cell lines to CDK4/6i. Although it was previously reported that MCF7 and T47D palbociclib resistant

derivatives showed increased sensitivity to JAK1/2 inhibition[21], these cells had also acquired *IL6* genomic amplification and significant upregulation of IL-6/STAT3 signaling, which would increase sensitivity to JAK1/2i. Here, upregulation of IL-6/STAT3 signaling was not seen in RNA-seq analyses. This suggests that canonical IFN signaling is associated with acquired resistance to CDK4/6 inhibition *in-vitro* but does not appear to drive growth or proliferation. Future work will be required to determine the mechanisms responsible for upregulated IFN signaling. In palbociclib resistant cell lines, De Angelis et al. found no association between the IFN response and loss of RB1 or upregulated DNA damage signaling, which have been previously associated with IFN induction[37]. Global DNA demethylation triggered by reduced expression or therapeutic inhibition of DNA methyltransferases (DNMT) induces "viral mimicry", which in turn stimulates IFN production[54–56]. A reduction of *DNMT1* in some palbociclib resistant models[37] has also been observed, therefore expression levels of additional DNMTs and their association with IFN induction may be explored in future studies. Interestingly, the progesterone receptor (PR) has been shown to interact with STAT1/2 to inhibit DNA binding and transcription of ISGs in T47D cells[57–59]. Therefore, loss of PR expression in CDK4/6i resistant models warrants further evaluation as a potential mechanism of IFN induction *in-vitro*.

While the inhibition of JAK/STAT signaling had no effect on resistant cells, acquired alterations in EGFR/HER, MAPK, and AKT/mTOR signaling pathways represent potential alternative therapeutic targets. Genomic sequencing uncovered low-level gains of *EGFR* in both MCF7 derivatives, as well as *BRAF* and *NF1* mutations in MCF7-PR and T47D-AR cells. To our knowledge, this is the first report of these alterations in CDK4/6i resistant cell lines. Upregulated EGFR expression was previously seen in a palbociclib resistant MCF7 cell line, though the mechanism for this was unclear[38]. Here we show that upregulated EGFR expression and activation can be attributed to acquired low-level *EGFR* genomic gains. These findings are clinically relevant as EGFR/HER and Ras-family molecular alterations have been acquired in CDK4/6i resistant tumours[29,31,33,60,61]. Together with recent clinical data, these results provide further support for the role of EGFR/HER-family and MAPK signaling in CDK4/6i resistance, and rationale for future evaluation of EGFR/HER/MAPK/CDK4/6i combinations in ER+/HER2- patients to delay onset of resistance.

Treatment options after CDK4/6i resistance also include targeting PI3K/AKT/mTOR signaling. PI3K signaling has been previously associated with CDK4/6i resistance in ER+/HER2- cell lines via activation of PDK1, AKT or loss of PTEN[23,29,34]. Several preclinical studies have shown that *PIK3CA*-mutant CDK4/6i resistant cell lines remain sensitive to PI3K pathway inhibitors[17,22,38], including PI3K-inhibitor alpelisib or mTORC1 inhibitor everolimus. These preclinical findings were recently validated in the phase II trial BYLieve, which demonstrated that alpelisib plus fulvestrant was effective in patients with *PIK3CA*-mutant advanced ER+/HER2- BC after progression on CDK4/6i[62]. Unlike alpelsib however, there are currently no biomarkers to select patients for everolimus treatment. Here, immunoblot analyses demonstrated increased 70S6K phosphorylation in both T47D derivatives, indicative of enhanced mTORC1 signaling, and provide further support for the evaluation of everolimus therapy after progression on CDK4/6i.

In summary, integration of genomic, transcriptomic, proteomic datasets from CDK4/6i resistant BC cell lines uncovered dysregulation of multiple signaling pathways and contributes to a growing understanding that mechanisms of CDK4/6i resistance are diverse. These findings offer unique therapeutic targets to prevent or overcome resistance. Intriguingly however, elevated IFN signaling was a common phenomenon across resistant models and warrants further investigation as a predictive biomarker of resistance to CDK4/6 inhibition.

Methods

Tissue Culture

600MPE and ZR75B cells were provided by Dr. Joe Gray (Oregon Health and Science University). HCC712 cells were provided by Dr. Adi Gazdar (University of Texas Southwestern Medical Center). KPL1 and EFM19 cell lines were provided by Dr. Tak Mak (University of Toronto). Other cell lines were obtained from the ATCC. Cells were maintained in RPMI-1640 Media (Gibco) or Dulbecco's Modified Eagle Medium (DMEM; Gibco) supplemented with 10% FBS at 37°C and humidified 5% CO_2. All cell lines were tested regularly for mycoplasma contamination (Venor GeM Classic Mycoplasma Detection Kit; Minerva Biolabs) and authenticated by STR analysis at the Centre for Applied Genomics at the Hospital for Sick Children (Toronto, Ontario).

Palbociclib (PR) and abemaciclib (AR) resistant cell lines were generated by culturing cells with increasing concentrations of CDK4/6i for 8 to 10 months, starting at 0.01µM and reaching a final concentration of 1µM. Resistant cell lines were maintained in media supplemented with 1µM CDK4/6i. CDK4/6i were omitted from growth media for 6 months to generate palbociclib-drug removed (PDR) and abemaciclib-drug removed (ADR) cell lines. All inhibitors were obtained from the Ontario Institute for Cancer Research's (OICR) compound library (Dr. Rima Al-Awar) and dissolved in dimethyl sulfoxide (DMSO; Sigma. Cells were maintained in drug-free medium for 24-48h prior to each experiment unless otherwise stated.

Flow Cytometry

Cells were treated +/- 0.5µM or 1µM CDK4/6i for 24h or 72h. Cells were fixed in ice-cold 80% ethanol for 1h at -20°C, washed and resuspended in 1x staining buffer (1x PBS pH7.4/0.6% NP-40/0.5mg/mL propidium iodide (Sigma)) for 30min at room temperature (RT), followed by addition of 1mg/mL RNase A (Sigma). Data were collected using a FACSCanto II Flow cytometer with FACSDiva software (BD Biosciences) and analyzed using FlowJo software v10.6.1 (BD Biosciences). Results represent a minimum of 10,000 events assayed for each sample. Experiments were performed twice in biological triplicate.

Cell viability assay

Cells were plated in 384-well plates at densities ranging from 200 to 3000 cells/well optimized for the untreated control cells to be 80-90% confluent at the endpoint of the experiment. Cells were plated using a Multi-drop Combi dispenser (Thermo Fisher Scientific). The following day, cells were treated with serial dilutions of each drug using an HP D300 digital compound dispenser (Tecan Systems). DMSO concentration did not exceed 0.5%. Cell viability was assessed at T0 and after 7 days of treatment using the CellTiter Glo Luminescent Cell Viability Assay (Promega) and the Wallac EnVision 2104 Multilabel Reader (PerkinElmer). Growth rate (GR) inhibition metrics, which control for different doubling times of the cell lines were used to generate normalized GR inhibition values[63]. GR values were determined using GraphPad Prism v5 software (GraphPad). Three independent experiments per cell line/inhibitor were performed.

Immunoblot analysis

Cells were treated +/- drug as indicated in figures. Cells were washed with ice-cold PBS (Gibco) and lysed in RIPA buffer: 10mM Tris-HCl pH8, 1mM EDTA pH8, 0.5mM EGTA pH8, 1% Triton X-100, 0.1% sodium deoxycholate, 0.1% SDS, 140mM NaCl, supplemented with protease (cOmplete, Mini, EDTA-free Protease Inhibitor Cocktail; Roche) and phosphatase inhibitors (HALT Phosphatase Inhibitor Cocktail; Thermo Fisher Scientific). Following lysis, samples were sonicated on ice for 5min (Bioruptor; Diagenode) and centrifuged

for 20min at 4°C. Protein lysate concentration was determined using the Pierce BCA Protein Assay Kit (Thermo Fisher Scientific). Samples were diluted to a final concentration of 1-2µg/µL in 5x Laemmili sample buffer: 250mM Tris-HCl pH6.8, 50% glycerol, 10% sodium dodecyl sulphate (SDS), 0.05% Bromophenol blue and 12.5% β-mercaptoethanol (BME). Samples were heated at 100°C for 5min, brought to RT, briefly centrifuged, and stored at -20°C.

A volume equivalent to 15-50µg of proteins was separated by SDS-PAGE electrophoresis on 4-20% Tris-glycine gels (Invitrogen). Gels were transferred onto polyvinylidene difluoride membranes (Bio-Rad). Membranes were blocked in 5% milk (Bio-Rad) or 5% BSA (Roche) for 1h at RT, followed by overnight incubation with primary antibodies at 4°C. The next day membranes were washed and probed with secondary antibodies for 1h at RT. Blots were developed using Clarity Western (ECL) Substrate (Bio-Rad). Visualization of proteins was performed using a ChemiDoc MP Imaging System and Image Lab software (Bio-Rad). A list of primary and secondary antibodies with their working conditions is provided in Supplementary Table S5. Immunoblots were performed in three independent experiments.

DNA sequencing

Cell line DNA was isolated using the QIAamp DNA Mini Kit (Qiagen). Sequencing libraries were prepared using the Oncomine Comprehensive Assay v3 (Thermo Fisher Scientific), which includes 161 cancer driver genes sequenced as either complete coding or hotspot regions for SNVs and indels, CNVs and gene fusions. Eight barcoded libraries were pooled onto one Ion 540 chip. Sequencing templates were prepared using the Ion Chef System (Thermo Fisher Scientific). Sequencing was performed using the Ion Torrent S5 (Thermo Fisher Scientific). Reads were processed using the Ion Reporter v5 (Thermo Fisher Scientific), which includes quality control, read trimming, and mapping to the human genome (hg19). A 5% lower confidence bound value > 4 was considered a CN gain. A 95% upper confidence bound < 1 was considered a CN deletion (assuming an expected ploidy of 2). Filtering of mutations was performed by Quang Trinh (Lincoln Stein lab, OICR) using an in-house pipeline adapted from previous work[64] to remove germline variants. Results were further filtered to remove mutations with p-values > 0.0001, variant allele frequency (VAF) < 5%, coverage < 250, and benign/likely benign status in the clinvar database. A colour-coded map of genomic alterations was constructed using the ComplexHeatmap package for R (v2.5.1)[65].

RNA sequencing

Total RNA was isolated using the RNeasy Mini-Kit (Qiagen). RNA concentration and quality was determined using the RNA 6000 Nano Assay and Agilent Bioanalyzer 2100 (Agilent Technologies). All samples had an RNA integrity number (RIN) greater than 9. External RNA Controls Consortium (ERCC) RNA Spike-In Mix 1 (Thermo Fisher Scientific) was added to each sample to assess library preparation and the lower limit of detection. rRNA was depleted from 2.5µg of total RNA using the RiboMinus Eukaryote Kit v2 (Ambion). Sequencing libraries were prepared using the Ion Total RNA-seq Kit v2 (Thermo Fisher Scientific) and Ion Xpress RNA-seq Barcode 01-16 Kit (Thermo Fisher Scientific). Sequencing templates were prepared using the Ion Chef System (Thermo Fisher Scientific). Three barcoded libraries were pooled onto one Ion 540 chip to generate approximately 20 million 100bp reads per sample. Sequencing was performed using the Ion Torrent S5 (Thermo Fisher Scientific). Automated quality control, read alignment and generation of raw gene counts were performed using Thermo Fisher's Torrent web server.

Differential gene expression analysis was performed using the edgeR package for R[66]. Genes were ranked by p-value and fold change. GSEA was performed using the Preranked tool within the GSEA 4.0 software (Broad Institute)[67] and a custom gene set developed by the Gary Bader lab (University of Toronto), available at http://download.baderlab.org/EM_Genesets/. Network analysis was visualized using

EnrichmentMap and Cytoscape v3.7.1 software[67]. The 52 genes commonly upregulated in all four CDK4/6i resistant cell lines (fold change>1.2, FDR<0.05) were selected for the IFN gene signature (IFN-sig).

RT-qPCR

RT-qPCR reactions were performed in 384-well plates using 20ng total RNA and the TaqMan Fast Virus 1-Step Master Mix (Thermo Fisher Scientific), according to the manufacturer's instructions. A list of TaqMan gene expression assays used in this study can be found in Supplementary Table S6. Reactions were performed in three technical replicates on the Applied Biosystems QuantStudio 6 Pro Real-Time PCR System instrument (Thermo Fisher Scientific) according to the following PCR program: 50°C for 5min (cDNA synthesis), 95°C for 20sec, and 40 cycles of 95°C for 3sec, 60°C for 1min. Relative transcript levels were calculated by the $2^{-\Delta\Delta Ct}$ method using the endogenous control gene, Ribosomal protein L37a (*RPL37A*). Three independent experiments were performed.

RPPA

Parental and CDK4/6i resistant cell lines were plated in biological triplicate. RPPA analysis was performed at the Center for Applied Proteomics and Molecular Medicine (George Mason University). Cells were lysed in extraction buffer composed of Tissue Protein Extraction agent (T-PER; Thermo Fisher), 300nM NaCl, 1mM Sodium Orthovanadate (Sigma), Pefabloc (Roche), 1µg/ml Aprotinin (Sigma), 1µg/ml Pepstatin A (Sigma) and 5µg/ml Leupeptin (Sigma). Protein concentration was determined using a Bradford assay, and samples diluted to a final concentration of 250µg/mL in T-PER buffer/1xSDS SB/2.5% BME. Samples were heated at 100°C for 5min, brought to RT, briefly centrifuged, and stored at -20°C until printing.
Lysates were printed and stained as previously described[68]. Briefly, lysates were printed (approx. 10nL per spot) on nitrocellulose coated slides (Grace Bio-Labs) using an Aushon 2470 Arrayer (Aushon Biosystems). Each sample was printed in triplicate. Standard curves of control cell lysates were also included for quality assurance purposes. Each slide was probed with one primary antibody. A complete list of primary antibodies and their working conditions can be found in Supplementary Table S7. Signal amplification was performed using a tyramide-based avidin/biotin amplification system (DakoCytomation) followed by streptavidin-conjugated IRDye 680 (LI-COR) for visualization. Total protein was measured using Sypro Ruby protein blot staining, according to the manufacturer's instructions (Molecular Probes). Images were acquired using a Tecan PowerScanner (Tecan) and analyzed using MicroVigene software v5.6 (Vigenetech). The final results represent negative control-subtracted and total protein normalized relative intensity values.

Gene Expression Datasets

NeoPalAna[41] data was downloaded from GEO (GSE93204) using the GEOquery R package[69]. A list of sensitive and resistant sample IDs was derived from previously published literature[41]. Cell line data from Marcotte et al.[40] were downloaded from Gene Expression Omnibus (GEO) (GSE73526). FASTQ files were aligned to hg38 and gene level count data generated using STAR v6.1[70]. Differential expression analysis was performed using the edgeR package for R[66]. Genes were ranked by p-value and fold change, and GSEA using genes from the IFN-sig was performed using the Preranked tool within the GSEA 4.0 software (Broad Institute)[67].

Statistical Analysis

Statistical significance was determined using an unpaired Student's t-test with p<=0.05 being regarded as statistically significant without correction for multiple testing, unless otherwise stated.

References

1. Finn, R. S. *et al.* Palbociclib and Letrozole in Advanced Breast Cancer. *New England Journal of Medicine* **375**, 1925–1936 (2016).

2. Hortobagyi, G. N. *et al.* Ribociclib as First-Line Therapy for HR-Positive, Advanced Breast Cancer. *N Engl J Med* **375**, 1738–1748 (2016).

3. Goetz, M. P. *et al.* MONARCH 3: Abemaciclib As Initial Therapy for Advanced Breast Cancer. *Journal of Clinical Oncology* **35**, 3638–3646 (2017).

4. Cristofanilli, M. *et al.* Fulvestrant plus palbociclib versus fulvestrant plus placebo for treatment of hormone-receptor-positive, HER2-negative metastatic breast cancer that progressed on previous endocrine therapy (PALOMA-3): final analysis of the multicentre, double-blind, phas. *Lancet Oncol* **17**, 425–439 (2016).

5. Sledge, G. W. *et al.* MONARCH 2: Abemaciclib in Combination With Fulvestrant in Women With HR+/HER2− Advanced Breast Cancer Who Had Progressed While Receiving Endocrine Therapy. *Journal of Clinical Oncology* **35**, 2875–2884 (2017).

6. Slamon, D. J. *et al.* Phase III Randomized Study of Ribociclib and Fulvestrant in Hormone Receptor–Positive, Human Epidermal Growth Factor Receptor 2–Negative Advanced Breast Cancer: MONALEESA-3. *Journal of Clinical Oncology* **36**, 2465–2472 (2018).

7. Slamon, D. J. *et al.* Overall Survival with Ribociclib plus Fulvestrant in Advanced Breast Cancer. *New England Journal of Medicine* **382**, 514–524 (2020).

8. Sledge, G. W. *et al.* The Effect of Abemaciclib Plus Fulvestrant on Overall Survival in Hormone Receptor–Positive, ERBB2-Negative Breast Cancer That Progressed on Endocrine Therapy—MONARCH 2. *JAMA Oncol* **6**, 116 (2020).

9. Slamon, D. J. *et al.* Ribociclib plus fulvestrant for postmenopausal women with hormone receptor-positive, human epidermal growth factor receptor 2-negative advanced breast cancer in the phase III randomized MONALEESA-3 trial: updated overall survival. *Annals of Oncology* **32**, 1015–1024 (2021).

10. Johnston, S. R. D. *et al.* Abemaciclib Combined With Endocrine Therapy for the Adjuvant Treatment of HR+, HER2−, Node-Positive, High-Risk, Early Breast Cancer (monarchE). *Journal of Clinical Oncology* **38**, 3987–3998 (2020).

11. Harbeck, N. *et al.* Adjuvant abemaciclib combined with endocrine therapy for high-risk early breast cancer: updated efficacy and Ki-67 analysis from the monarchE study. *Annals of Oncology* **32**, 1571–1581 (2021).

12. Finn, R. S. *et al.* PD 0332991, a selective cyclin D kinase 4/6 inhibitor, preferentially inhibits proliferation of luminal estrogen receptor-positive human breast cancer cell lines in vitro. *Breast Cancer Research* **11**, R77 (2009).

13. Dean, J. L., Thangavel, C., McClendon, a K., Reed, C. a & Knudsen, E. S. Therapeutic CDK4/6 inhibition in breast cancer: key mechanisms of response and failure. *Oncogene* **29**, 4018–4032 (2010).

14. Dean, J. L. *et al.* Therapeutic response to CDK4/6 inhibition in breast cancer defined by ex vivo analyses of human tumors. *Cell Cycle* **11**, 2756–2761 (2012).

15. Gelbert, L. M. *et al.* Preclinical characterization of the CDK4/6 inhibitor LY2835219: in-vivo cell cycle-dependent/independent anti-tumor activities alone/in combination with gemcitabine. *Invest New Drugs* **32**, 825–837 (2014).

16. Malorni, L. *et al.* A gene expression signature of retinoblastoma loss-of-function is a predictive biomarker of resistance to palbociclib in breast cancer cell lines and is prognostic in patients with ER positive early breast cancer. *Oncotarget* **7**, 68012–68022 (2016).

17. Herrera-Abreu, M. T. *et al.* Early Adaptation and Acquired Resistance to CDK4/6 Inhibition in Estrogen Receptor–Positive Breast Cancer. *Cancer Res* **76**, 2301–2313 (2016).

18. Guarducci, C. *et al.* Cyclin E1 and Rb modulation as common events at time of resistance to palbociclib in hormone receptor-positive breast cancer. *NPJ Breast Cancer* **4**, 38 (2018).

19. Li, Z. *et al.* Loss of the FAT1 Tumor Suppressor Promotes Resistance to CDK4/6 Inhibitors via the Hippo Pathway. *Cancer Cell* **34**, 893-905.e8 (2018).

20. Condorelli, R. *et al.* Polyclonal RB1 mutations and acquired resistance to CDK 4/6 inhibitors in patients with metastatic breast cancer. *Annals of Oncology* **29**, 640–645 (2018).

21. Kettner, N. M. *et al.* Combined Inhibition of STAT3 and DNA Repair in Palbociclib-Resistant ER-Positive Breast Cancer. *Clinical Cancer Research* **25**, 3996–4013 (2019).

22. O'Brien, N. A. *et al.* Targeting activated PI3K/mTOR signaling overcomes acquired resistance to CDK4/6-based therapies in preclinical models of hormone receptor-positive breast cancer. *Breast Cancer Research* **22**, 89 (2020).

23. Costa, C. *et al.* PTEN Loss Mediates Clinical Cross-Resistance to CDK4/6 and PI3Kα Inhibitors in Breast Cancer. *Cancer Discov* **10**, 72–85 (2020).

24. Palafox, M. *et al.* High p16 expression and heterozygous RB1 loss are biomarkers for CDK4/6 inhibitor resistance in ER+ breast cancer. *Nat Commun* **13**, 5258 (2022).

25. Yang, C. *et al.* Acquired CDK6 amplification promotes breast cancer resistance to CDK4/6 inhibitors and loss of ER signaling and dependence. *Oncogene* **36**, 2255–2264 (2017).

26. Cornell, L., Wander, S. A., Visal, T., Wagle, N. & Shapiro, G. I. MicroRNA-Mediated Suppression of the TGF-β Pathway Confers Transmissible and Reversible CDK4/6 Inhibitor Resistance. *Cell Rep* **26**, 2667-2680.e7 (2019).

27. Griffiths, J. I. *et al.* Serial single-cell genomics reveals convergent subclonal evolution of resistance as patients with early-stage breast cancer progress on endocrine plus CDK4/6 therapy. *Nat Cancer* **2**, 658–671 (2021).

28. Turner, N. C. *et al.* Cyclin E1 Expression and Palbociclib Efficacy in Previously Treated Hormone Receptor–Positive Metastatic Breast Cancer. *Journal of Clinical Oncology* **37**, 1169–1178 (2019).

29. Wander, S. A. *et al.* The Genomic Landscape of Intrinsic and Acquired Resistance to Cyclin-Dependent Kinase 4/6 Inhibitors in Patients with Hormone Receptor–Positive Metastatic Breast Cancer. *Cancer Discov* **10**, 1174–1193 (2020).

30. Formisano, L. *et al.* Aberrant FGFR signaling mediates resistance to CDK4/6 inhibitors in ER+ breast cancer. *Nat Commun* **10**, 1373 (2019).

31. Mao, P. *et al.* Acquired FGFR and FGF Alterations Confer Resistance to Estrogen Receptor (ER) Targeted Therapy in ER + Metastatic Breast Cancer. *Clinical Cancer Research* **26**, 5974–5989 (2020).

32. O'Leary, B. *et al.* Circulating Tumor DNA Markers for Early Progression on Fulvestrant With or Without Palbociclib in ER+ Advanced Breast Cancer. *JNCI: Journal of the National Cancer Institute* **113**, 309–317 (2021).

33. Nayar, U. *et al.* Acquired HER2 mutations in ER+ metastatic breast cancer confer resistance to estrogen receptor–directed therapies. *Nat Genet* **51**, 207–216 (2019).

34. Jansen, V. M. *et al.* Kinome-Wide RNA Interference Screen Reveals a Role for PDK1 in Acquired Resistance to CDK4/6 Inhibition in ER-Positive Breast Cancer. *Cancer Res* **77**, 2488–2499 (2017).

35. Abu-Khalaf, M. M. *et al.* AKT/mTOR signaling modulates resistance to endocrine therapy and CDK4/6 inhibition in metastatic breast cancers. *NPJ Precis Oncol* **7**, 18 (2023).

36. de Leeuw, R. *et al.* MAPK Reliance via Acquired CDK4/6 Inhibitor Resistance in Cancer. *Clinical Cancer Research* **24**, 4201–4214 (2018).

37. De Angelis, C. *et al.* Activation of the IFN Signaling Pathway is Associated with Resistance to CDK4/6 Inhibitors and Immune Checkpoint Activation in ER-Positive Breast Cancer. *Clinical Cancer Research* **27**, 4870–4882 (2021).

38. Pancholi, S. *et al.* Tumour kinome re-wiring governs resistance to palbociclib in oestrogen receptor positive breast cancers, highlighting new therapeutic modalities. *Oncogene* **39**, 4781–4797 (2020).

39. O'Brien, N. *et al.* Preclinical Activity of Abemaciclib Alone or in Combination with Antimitotic and Targeted Therapies in Breast Cancer. *Mol Cancer Ther* **17**, 897–907 (2018).

40. Marcotte, R. *et al.* Functional Genomic Landscape of Human Breast Cancer Drivers, Vulnerabilities, and Resistance. *Cell* **164**, 293–309 (2016).

41. Ma, C. X. *et al.* NeoPalAna: Neoadjuvant Palbociclib, a Cyclin-Dependent Kinase 4/6 Inhibitor, and Anastrozole for Clinical Stage 2 or 3 Estrogen Receptor–Positive Breast Cancer. *Clinical Cancer Research* **23**, 4055–4065 (2017).

42. Musella, M., Galassi, C., Manduca, N. & Sistigu, A. The Yin and Yang of Type I IFNs in Cancer Promotion and Immune Activation. *Biology (Basel)* **10**, 856 (2021).

43. Zitvogel, L., Galluzzi, L., Kepp, O., Smyth, M. J. & Kroemer, G. Type I interferons in anticancer immunity. *Nat Rev Immunol* **15**, 405–414 (2015).

44. Brett, J. O., Herman, P. E., Mayer, E. L., Bardia, A. & Wander, S. A. Mechanisms of Resistance to CDK4/6 Inhibitors in Hormone Receptor-Positive (HR +) Breast Cancer: Spotlight on Convergent CDK6 Upregulation and Immune Signaling. *Curr Breast Cancer Rep* **14**, 222–232 (2022).

45. Choi, H. J. *et al.* Targeting interferon response genes sensitizes aromatase inhibitor resistant breast cancer cells to estrogen-induced cell death. *Breast Cancer Research* **17**, 6 (2015).

46. Lui, A. J. *et al.* IFITM1 suppression blocks proliferation and invasion of aromatase inhibitor-resistant breast cancer in vivo by JAK/STAT-mediated induction of p21. *Cancer Lett* **399**, 29–43 (2017).

47. Post, A. E. M. *et al.* Interferon-Stimulated Genes Are Involved in Cross-resistance to Radiotherapy in Tamoxifen-Resistant Breast Cancer. *Clinical Cancer Research* **24**, 3397–3408 (2018).

48. Benci, J. L. *et al.* Opposing Functions of Interferon Coordinate Adaptive and Innate Immune Responses to Cancer Immune Checkpoint Blockade. *Cell* **178**, 933-948.e14 (2019).

49. Benci, J. L. *et al.* Tumor Interferon Signaling Regulates a Multigenic Resistance Program to Immune Checkpoint Blockade. *Cell* **167**, 1540-1554.e12 (2016).

50. Jacquelot, N. *et al.* Sustained Type I interferon signaling as a mechanism of resistance to PD-1 blockade. *Cell Res* **29**, 846–861 (2019).

51. Schuster, E. F. *et al.* Abstract PS5-01: Biomarkers of resistance to palbociclib in ER+ primary breast cancer in the PALLET trial. *Cancer Res* **81**, PS5-01-PS5-01 (2021).

52. Schuster, E. F. *et al.* Abstract PD15-03: Overlapping molecular features (proliferation, immune signatures and TP53 mutations) associated with palbociclib resistance inER+HER2- primary breast cancer. *Cancer Res* **82**, PD15-03-PD15-03 (2022).

53. Freeman-Cook, K. *et al.* Expanding control of the tumor cell cycle with a CDK2/4/6 inhibitor. *Cancer Cell* **39**, 1404-1421.e11 (2021).

54. Goel, S. *et al.* CDK4/6 inhibition triggers anti-tumour immunity. *Nature* **548**, 471–475 (2017).

55. Chiappinelli, K. B. *et al.* Inhibiting DNA Methylation Causes an Interferon Response in Cancer via dsRNA Including Endogenous Retroviruses. *Cell* **162**, 974–986 (2015).

56. Roulois, D. *et al.* DNA-Demethylating Agents Target Colorectal Cancer Cells by Inducing Viral Mimicry by Endogenous Transcripts. *Cell* **162**, 961–973 (2015).

57. Goodman, M. L. *et al.* Progesterone Receptor Attenuates STAT1-Mediated IFN Signaling in Breast Cancer. *The Journal of Immunology* **202**, 3076–3086 (2019).

58. Walter, K. R., Balko, J. M. & Hagan, C. R. Progesterone receptor promotes degradation of STAT2 to inhibit the interferon response in breast cancer. *Oncoimmunology* **9**, 1758547 (2020).

59. Walter, K. R. *et al.* Interferon-Stimulated Genes Are Transcriptionally Repressed by PR in Breast Cancer. *Molecular Cancer Research* **15**, 1331–1340 (2017).

60. O'Leary, B. *et al.* The Genetic Landscape and Clonal Evolution of Breast Cancer Resistance to Palbociclib plus Fulvestrant in the PALOMA-3 Trial. *Cancer Discov* **8**, 1390–1403 (2018).

61. Drago, J. Z. *et al.* FGFR1 Amplification Mediates Endocrine Resistance but Retains TORC Sensitivity in Metastatic Hormone Receptor–Positive (HR +) Breast Cancer. *Clinical Cancer Research* **25**, 6443–6451 (2019).

62. Rugo, H. S. *et al.* Alpelisib plus fulvestrant in PIK3CA-mutated, hormone receptor-positive advanced breast cancer after a CDK4/6 inhibitor (BYLieve): one cohort of a phase 2, multicentre, open-label, non-comparative study. *Lancet Oncol* **22**, 489–498 (2021).

63. Hafner, M., Niepel, M., Chung, M. & Sorger, P. K. Growth rate inhibition metrics correct for confounders in measuring sensitivity Ato cancer drugs. *Nat Methods* **13**, 521–527 (2016).

64. Kalatskaya, I. *et al.* ISOWN: accurate somatic mutation identification in the absence of normal tissue controls. *Genome Med* **9**, 59 (2017).

65. Gu, Z., Eils, R. & Schlesner, M. Complex heatmaps reveal patterns and correlations in multidimensional genomic data. *Bioinformatics* **32**, 2847–9 (2016).

66. Robinson, M. D., McCarthy, D. J. & Smyth, G. K. edgeR: a Bioconductor package for differential expression analysis of digital gene expression data. *Bioinformatics* **26**, 139–40 (2010).

67. Reimand, J. *et al.* Pathway enrichment analysis and visualization of omics data using g:Profiler, GSEA, Cytoscape and EnrichmentMap. *Nat Protoc* **14**, 482–517 (2019).

68. Wulfkuhle, J. D. *et al.* Evaluation of the HER/PI3K/AKT Family Signaling Network as a Predictive Biomarker of Pathologic Complete Response for Patients With Breast Cancer Treated With Neratinib in the I-SPY 2 TRIAL. *JCO Precis Oncol* 1–20 (2018) doi:10.1200/PO.18.00024.

69. Davis, S. & Meltzer, P. S. GEOquery: a bridge between the Gene Expression Omnibus (GEO) and BioConductor. *Bioinformatics* **23**, 1846–1847 (2007).

70. Dobin, A. *et al.* STAR: ultrafast universal RNA-seq aligner. *Bioinformatics* **29**, 15–21 (2013).

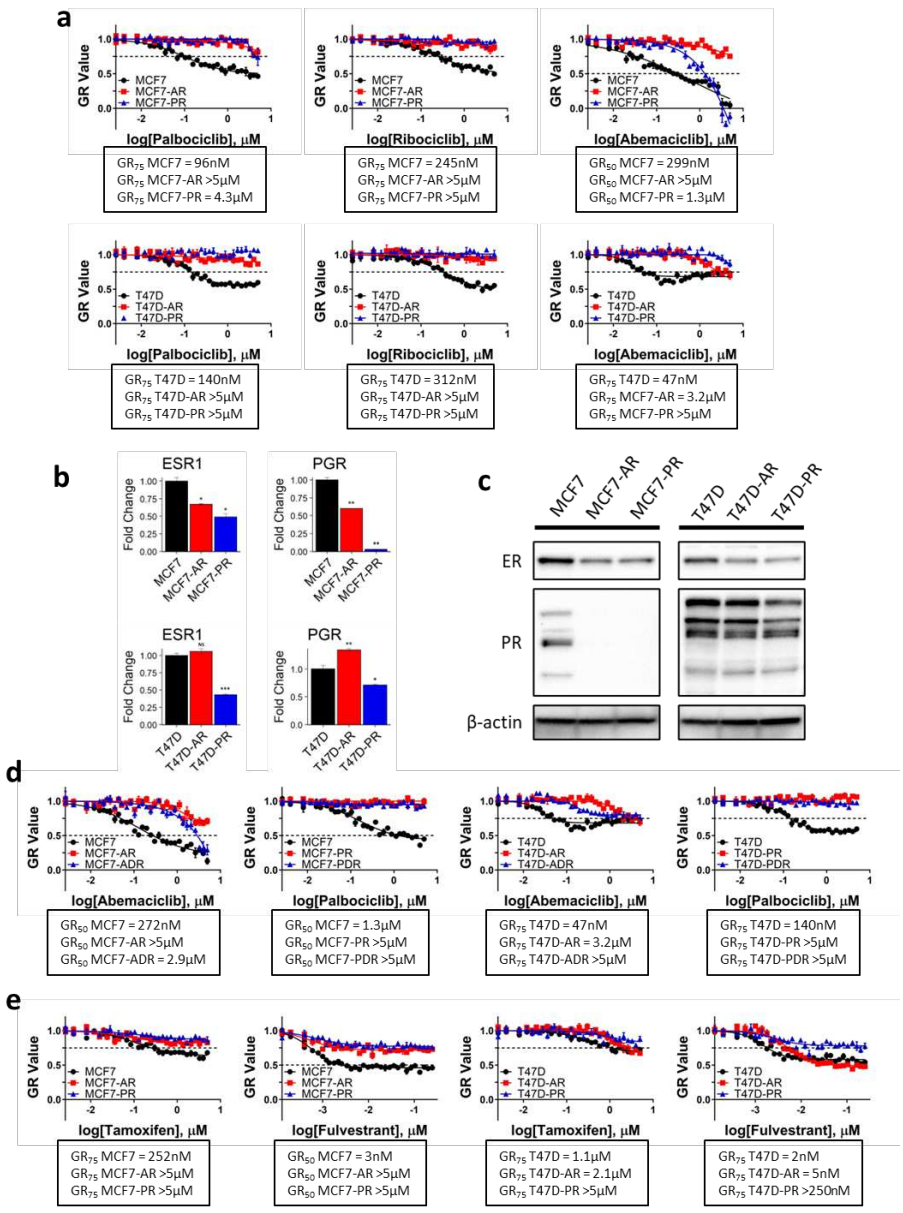

Fig. 1: Diminished response to CDK4/6i and endocrine therapy in CDK4/6i resistant derivatives. a Dose-response curves from parental (black), AR (red) and PR (blue) cell lines treated for 7 days with increasing concentrations of palbociclib, ribociclib or abemaciclib. Cell viability was measured via CellTiter Glo. Each data point represents the average of values obtained from three independent experiments +/- SEM. Dashed lines represent GR75 or GR50 values as indicated on the y-axis. **b-c** Parental and resistant cells were cultured in untreated media for 48h. **b** mRNA levels of the indicated genes were measured by RT-qPCR. Each bar represents mean fold change relative to the parental cell line +/- SEM from three independent experiments (***, $P < 0.001$; **, $P < 0.01$; *, $P < 0.05$). **c** Protein lysates were analyzed by immunoblot with the indicated antibodies. Three independent experiments were performed. Results from one representative experiment are shown. **d** Dose-response curves in parental (black), AR (red) and PR (blue) cell lines treated for 7 days with increasing concentrations of drug. **e** Dose-response curves from parental (black), resistant (red) and drug removed (blue) cell lines treated for 7 days with increasing concentrations of palbociclib or abemaciclib.

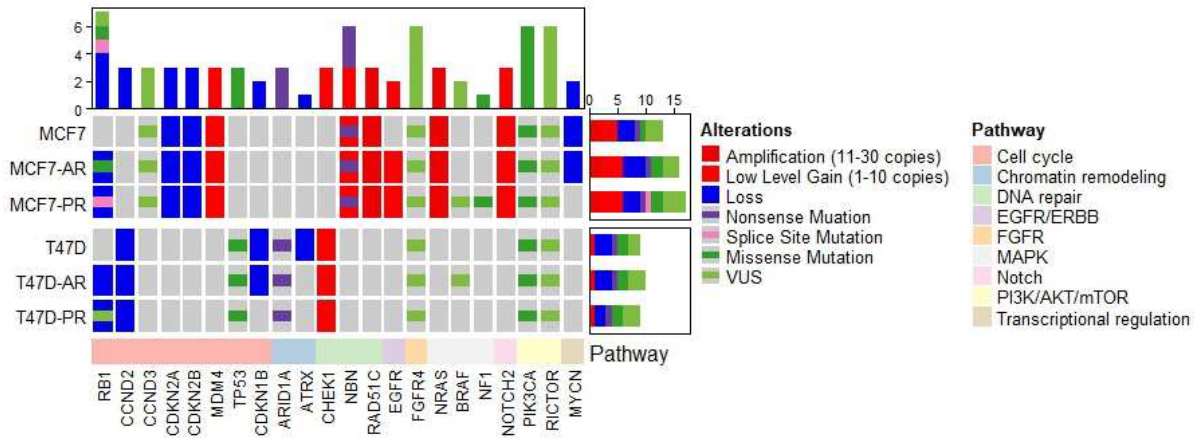

Fig. 2: Acquired genomic alterations in cell cycle, EGFR and MAPK pathway components in CDK4/6i resistant derivatives.

Summary of Oncomine sequencing analyses. Heatmap representing genomic alterations by signaling pathway (gray = no alteration, VUS = variant of unknown significance). Top bar chart, total number of alterations in each gene. Right bar chart, total number of alterations in each cell line.

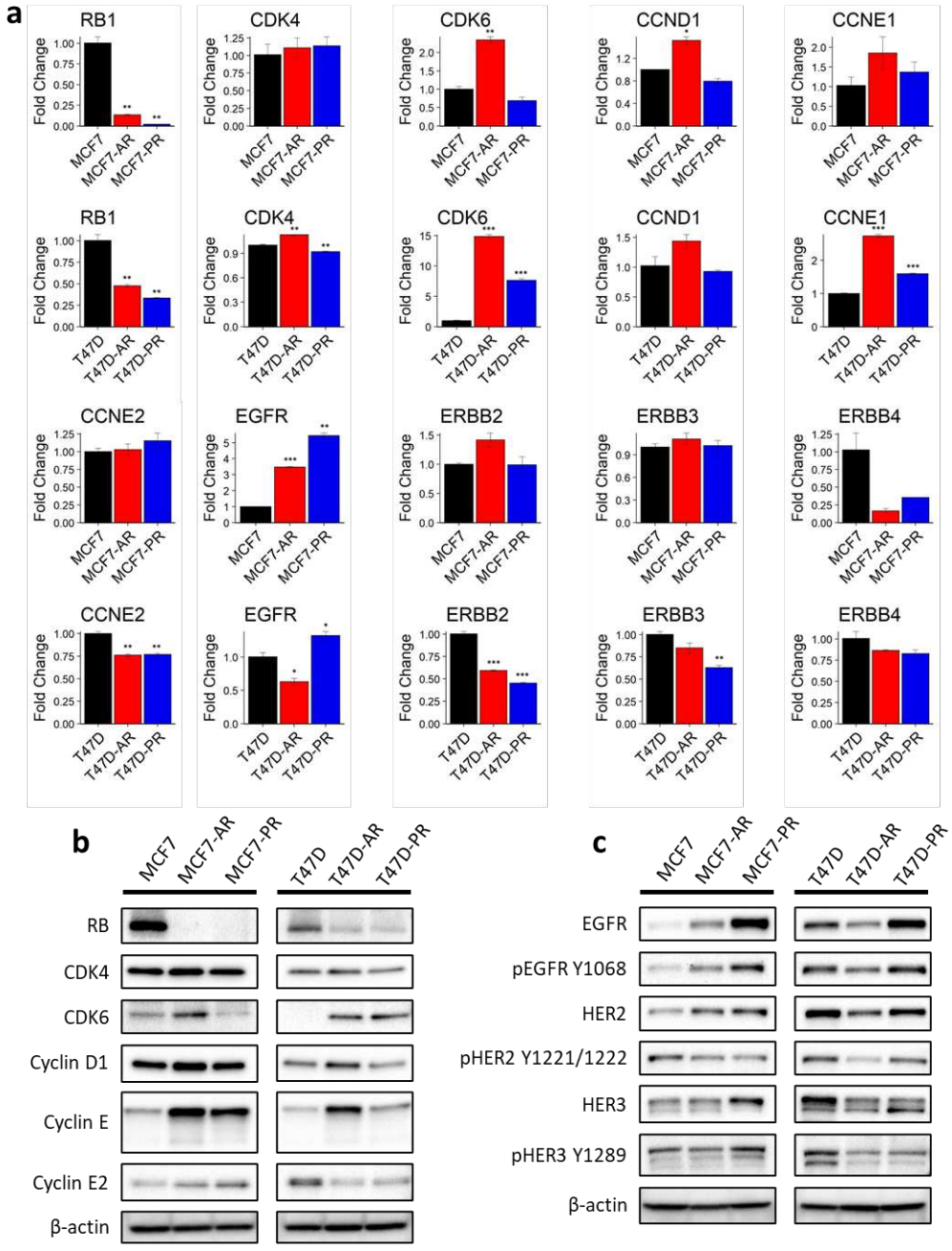

Fig. 3: Dysregulation of cell cycle and EGFR/HER-family genes in CDK4/6i resistant derivatives. a-c Parental and resistant cells were cultured in untreated media for 48h. **a** mRNA levels of the indicated genes were measured by RT-qPCR. Each bar represents mean fold change relative to the parental cell line +/- SEM from three independent experiments (***, $P < 0.001$; **, $P < 0.01$; *, $P < 0.05$). **b-c** Protein lysates were analyzed by immunoblot with the indicated antibodies. Three independent experiments were performed. Results from one representative experiment are shown.

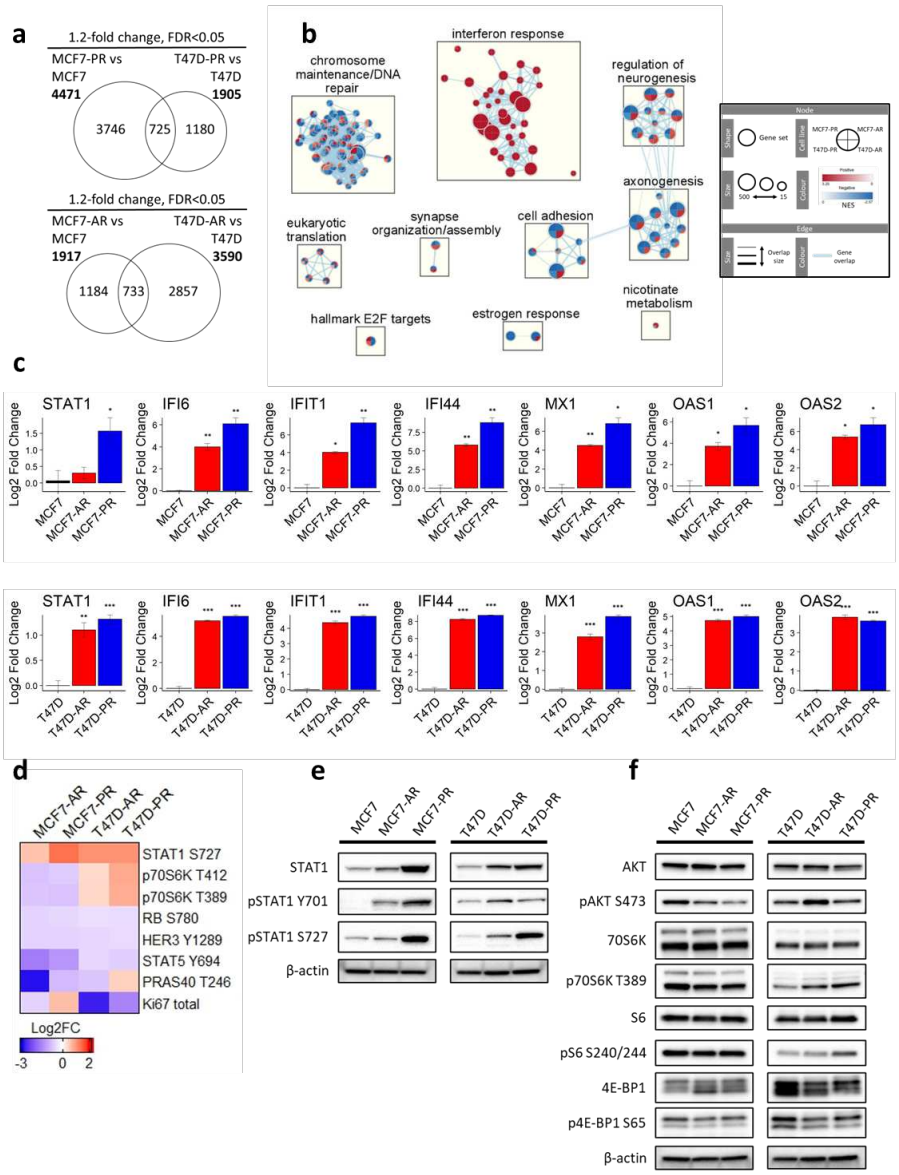

Fig. 4: Dysregulation of IFN and AKT/mTORC1 signaling in CDK4/6i resistant derivatives. a-f Parental and resistant cells were cultured in untreated media for 48h. mRNA expression was analyzed by RNA-seq. **a** Venn diagrams showing overlap of genes differentially expressed in palbociclib resistant models (top) and abemaciclib resistant models (bottom) compared to parental cell lines. **b** Enrichment map of gene sets significantly upregulated (red) or downregulated (blue) in CDK4/6i resistant cells compared to parental cells. Each node (circle) represents a gene set. Edges (blue lines) represent the number of genes overlapping between two gene sets. Node size corresponds to number of genes in each gene set. Colour corresponds to normalized enrichment score (NES). Similar gene sets were clustered together to highlight biological themes. **c** mRNA levels of the indicated genes were measured by RT-qPCR. Each bar represents mean fold change relative to the parental cell line +/- SEM from three independent experiments (***, P < 0.001; **, P < 0.01; *, P < 0.05). **d** Protein lysates were analyzed by RPPA with the indicated antibodies. Protein expression represents the average of values obtained from three biological replicates. Heat map showing Log2 fold changes in protein expression in resistant cell lines compared to parental cell lines. **e-f** Protein lysates were analyzed by immunoblot with the indicated antibodies. Three independent experiments were performed. Results from one representative experiment are shown.

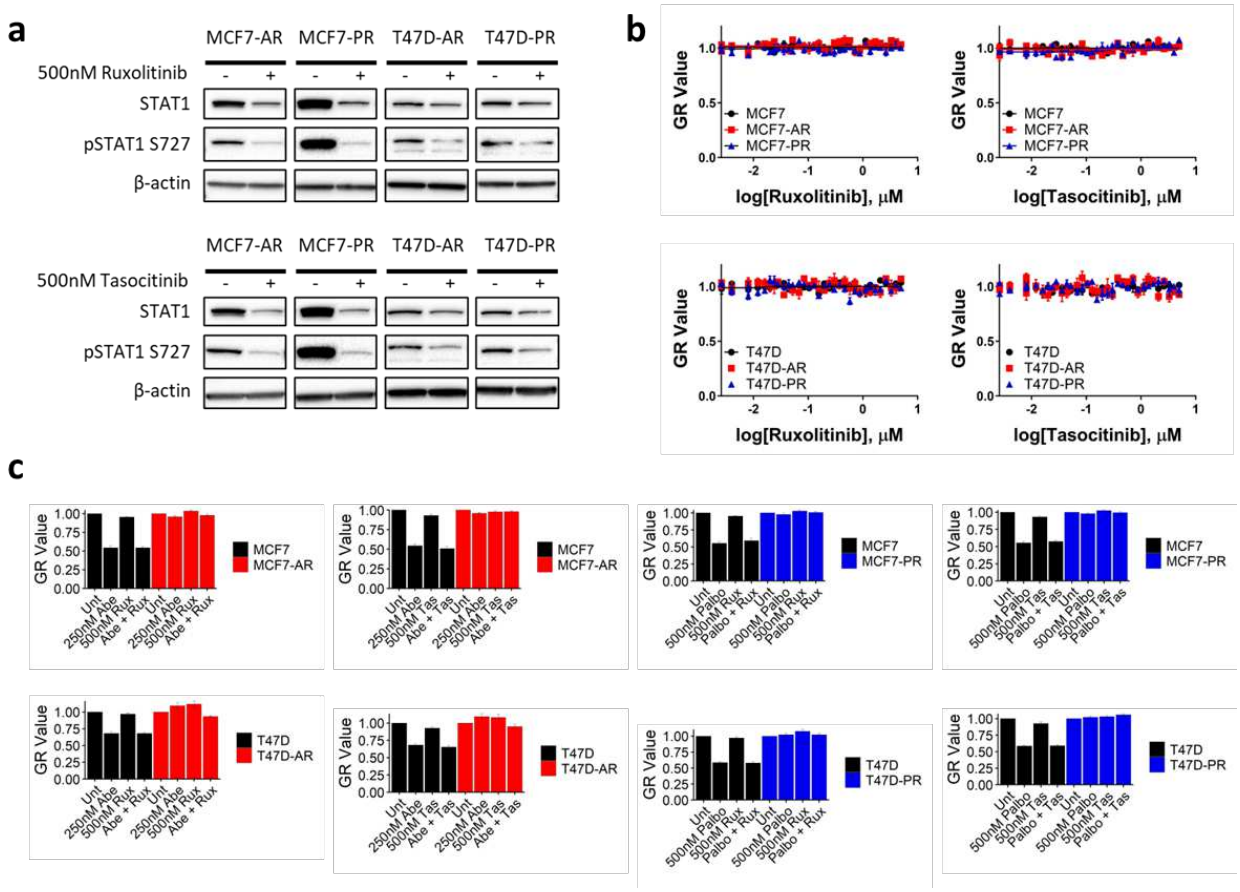

Fig. 5: JAK1/2 inhibition does not affect cell viability of CDK4/6i resistant derivatives. a Resistant cells were treated +/- the indicated concentrations of ruxolitinib or tasocitinib for 96h. Protein lysates were analyzed by immunoblot with the indicated antibodies. Three independent experiments were performed. Results from one representative experiment are shown. **b** Dose-response curves in parental (black), AR (red) and PR (blue) cell lines treated for 7 days with increasing concentrations of drug. Cell viability was measured via CellTiter Glo. Each data point represents the average of values obtained from three independent experiments +/- SEM. **c** Parental and resistant cell lines were treated with the indicated drugs for 7 days. Cell viability was measured via CellTiter Glo. Each bar represents mean GR value +/- SEM from two independent experiments performed in triplicate.

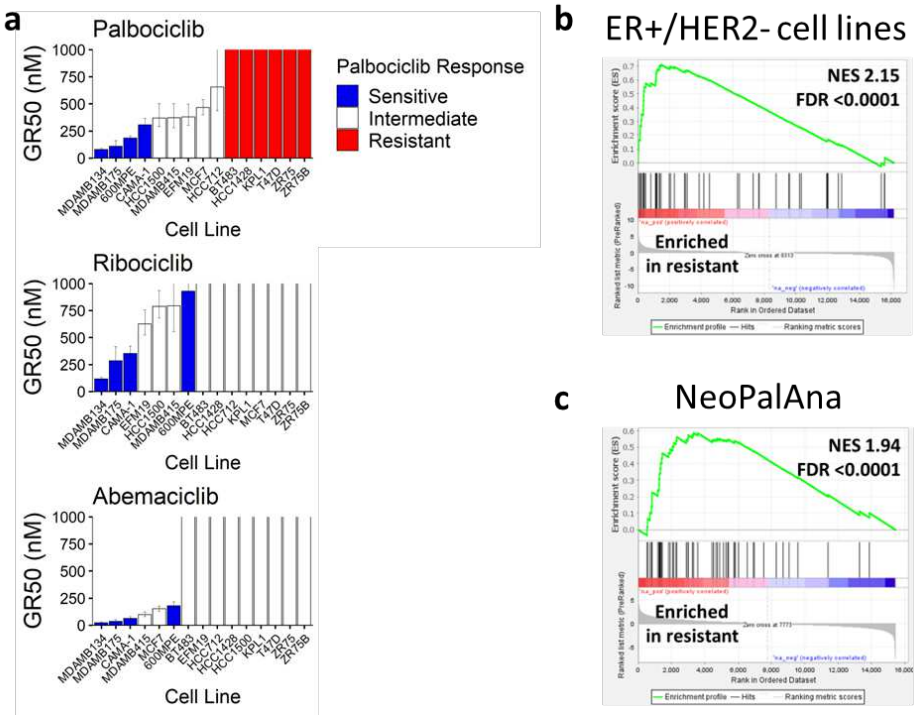

Fig. 6: IFN-sig expression enriched in palbociclib resistant ER+/HER2- breast cancer cell lines and patient tumours. a Cells were treated for 7 days with increasing concentrations of inhibitor. Cell viability was measured via CellTiter Glo. Each bar represents mean GR50 value +/- SEM from three independent experiments. **b** Differential gene expression was performed using publicly available RNA-seq data[40]. GSEA plot indicating that IFN-sig expression is enriched in palbociclib resistant ER+/HER2- cell lines. **c** GSEA plot indicating that IFN-sig expression is enriched in palbociclib resistant tumours from the NeoPalAna dataset[41]. NES = normalized enrichment score. FDR = false discovery rate.

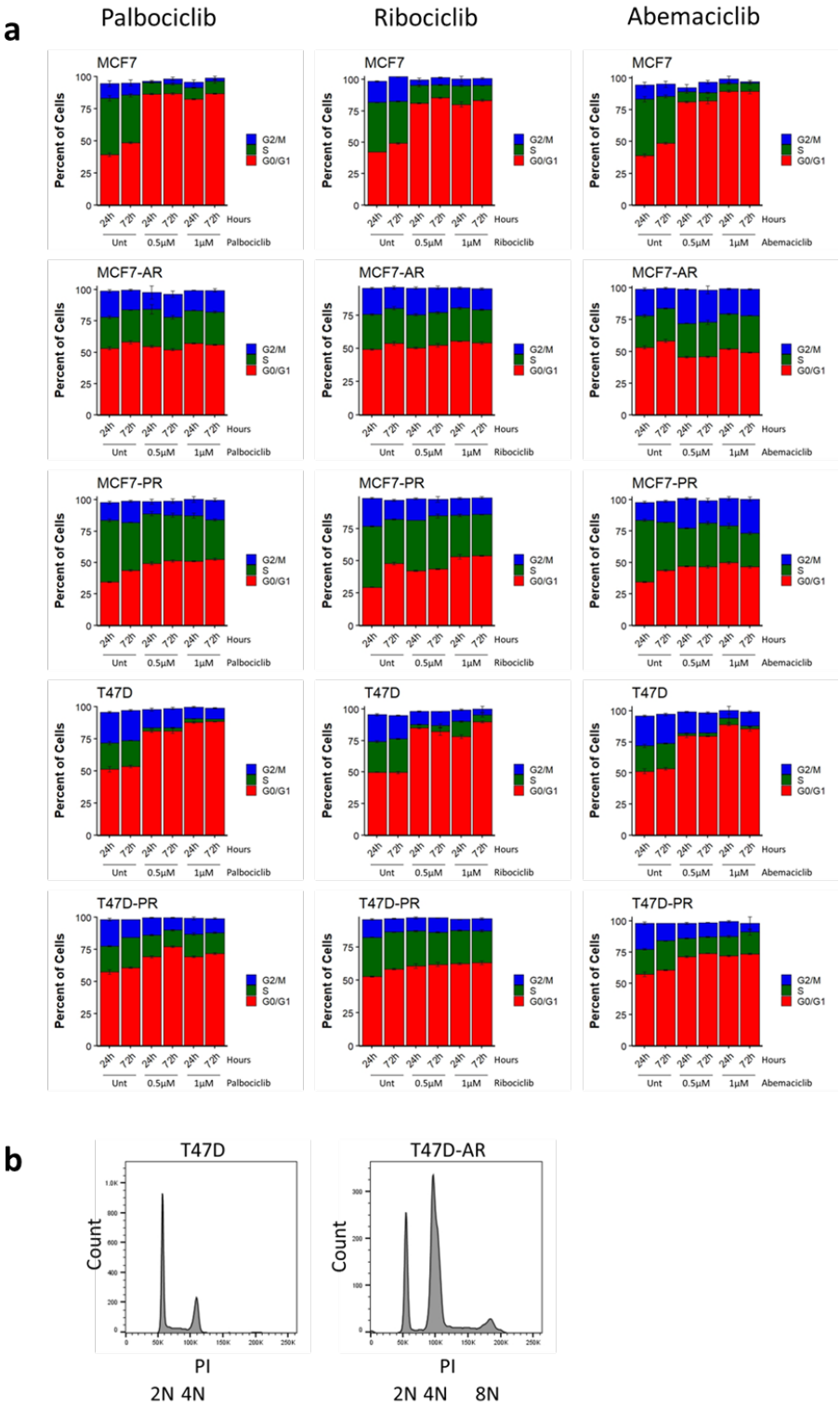

Supplementary Fig. 1: Palbociclib, ribociclib and abemaciclib increase G0/G1-phase arrest in parental cells compared to their CDK4/6i resistant derivatives. a Parental and resistant cells were treated +/- 0.5μM or 1μM CDK4/6i for 24h and 72h. Cell cycle analysis was performed using propidium iodine (PI) staining. Results are reported as mean percentage cell cycle distribution +/- SEM. Experiments were performed twice. Results of one representative experiment are shown. **b** Cell cycle analysis was performed using PI staining. PI histogram plots of untreated T47D and T47D-AR cells.

Supplementary Table S1 Cell line mutations identified by Oncomine sequencing.

Cell Line	Gene	Coding	Protein	VAF	p-value	Coverage	Genotype	Clinvar	Mutation Type
MCF7	CCND3	c.775T>G	p.Ser259Ala	46.69	0	1994	HETEROZYGOUS	VUS	VUS
MCF7	FGFR4	c.1162G>A	p.Gly388Arg	74.27	0	1982	HETEROZYGOUS	VUS	VUS
MCF7	NBN	c.127C>T	p.Arg43Ter	74.84	0	1999	HETEROZYGOUS	Pathogenic	nonsense
MCF7	NBN	c.974C>A	p.Pro325His	12.87	8.21E-97	1927	HETEROZYGOUS	VUS	VUS
MCF7	PIK3CA	c.1633G>A	p.Glu545Lys	46.85	0	2000	HETEROZYGOUS	Pathogenic	missense
MCF7	RICTOR	c.2510C>T	p.Ser837Phe	23.24	1.78E-287	1971	HETEROZYGOUS	VUS	VUS
MCF7-AR	CCND3	c.775T>G	p.Ser259Ala	33.67	0	1999	HETEROZYGOUS	VUS	VUS
MCF7-AR	FGFR4	c.1162G>A	p.Gly388Arg	75.51	0	1993	HETEROZYGOUS	VUS	VUS
MCF7-AR	NBN	c.127C>T	p.Arg43Ter	72.07	0	1998	HETEROZYGOUS	Pathogenic	nonsense
MCF7-AR	NBN	c.974C>A	p.Pro325His	13.2	2.00E-105	2000	HETEROZYGOUS	VUS	VUS
MCF7-AR	PIK3CA	c.1633G>A	p.Glu545Lys	64.13	0	1999	HETEROZYGOUS	Pathogenic	missense
MCF7-AR	RB1	c.1700C>T	p.Ser567Leu	98.73	1.12E-244	157	HOMOZYGOUS	Pathogenic	missense
MCF7-AR	RICTOR	c.2510C>T	p.Ser837Phe	23.4	1.05E-296	2000	HETEROZYGOUS	VUS	VUS
MCF7-PR	BRAF	c.2128-3GT>T	p.?	14.19	3.41E-20	430	HETEROZYGOUS	VUS	VUS
MCF7-PR	CCND3	c.775T>G	p.Ser259Ala	33.85	0	1994	HETEROZYGOUS	VUS	VUS
MCF7-PR	FGFR4	c.1162G>A	p.Gly388Arg	72.28	0	1991	HETEROZYGOUS	VUS	VUS
MCF7-PR	NBN	c.127C>T	p.Arg43Ter	71.12	0	1998	HETEROZYGOUS	Pathogenic	nonsense
MCF7-PR	NBN	c.974C>A	p.Pro325His	11.05	2.83E-74	2000	HETEROZYGOUS	VUS	VUS
MCF7-PR	NF1	c.5561T>C	p.Leu1854Pro	47.02	0	1997	HETEROZYGOUS	Pathogenic	missense
MCF7-PR	PIK3CA	c.1633G>A	p.Glu545Lys	66.57	0	1998	HETEROZYGOUS	Pathogenic	missense
MCF7-PR	RB1	c.1216-2A>G	p.?	93.39	0	771	HETEROZYGOUS	Pathogenic	spliceacceptor
MCF7-PR	RICTOR	c.2510C>T	p.Ser837Phe	25.51	0	1999	HETEROZYGOUS	VUS	VUS
T47D	ARID1A	c.2830C>T	p.Gln944Ter	100	0	497	HOMOZYGOUS	Pathogenic	nonsense
T47D	FGFR4	c.1162G>A	p.Gly388Arg	32.78	0	1995	HETEROZYGOUS	VUS	VUS
T47D	PIK3CA	c.3140A>G	p.His1047Arg	85.85	0	2000	HETEROZYGOUS	Pathogenic	missense
T47D	RICTOR	c.2510C>T	p.Ser837Phe	99.34	0	1674	HOMOZYGOUS	VUS	VUS
T47D	TP53	c.580C>T	p.Leu194Phe	100	0	913	HOMOZYGOUS	Pathogenic	missense

T47D-AR	ARID1A	c.2830C>T	p.Gln944Ter	91.56	0	1055	HETEROZYGOUS	Pathogenic	nonsense
T47D-AR	BRAF	c.2128-3GT>T	p.?	14.57	3.54E-11	254	HETEROZYGOUS	VUS	VUS
T47D-AR	FGFR4	c.1162G>A	p.Gly388Arg	28.84	0	1994	HETEROZYGOUS	VUS	VUS
T47D-AR	PIK3CA	c.3140A>G	p.His1047Arg	90.95	0	2000	HETEROZYGOUS	Pathogenic	missense
T47D-AR	RICTOR	c.2510C>T	p.Ser837Phe	99.3	0	2000	HOMOZYGOUS	VUS	VUS
T47D-AR	TP53	c.580C>T	p.Leu194Phe	100	0	1852	HOMOZYGOUS	Pathogenic	missense
T47D-PR	ARID1A	c.2830C>T	p.Gln944Ter	91.82	0	1210	HETEROZYGOUS	Pathogenic	nonsense
T47D-PR	FGFR4	c.1162G>A	p.Gly388Arg	39.93	0	1996	HETEROZYGOUS	VUS	VUS
T47D-PR	PIK3CA	c.3140A>G	p.His1047Arg	91.3	0	2000	HETEROZYGOUS	Pathogenic	missense
T47D-PR	RB1	179insA	p.Leu60fs	8.5	2.25E-18	812	HETEROZYGOUS	VUS	VUS
T47D-PR	RICTOR	c.2510C>T	p.Ser837Phe	99.2	0	1999	HOMOZYGOUS	VUS	VUS
T47D-PR	TP53	c.580C>T	p.Leu194Phe	99.85	0	1994	HOMOZYGOUS	Pathogenic	missense

Supplementary Table S2 MSigDB HALLMARK gene sets significantly up- and downregulated in CDK4/6i resistant cell lines.

Upregulated Gene Sets in MCF7-AR vs MCF7					
MSigDB HALLMARK	**SIZE**	**ES**	**NES**	**NOM p-val**	**FDR q-val**
HALLMARK_INTERFERON_ALPHA_RESPONSE	87	0.84	2.88	0.000	0.000
HALLMARK_INTERFERON_GAMMA_RESPONSE	155	0.76	2.79	0.000	0.000
HALLMARK_CHOLESTEROL_HOMEOSTASIS	69	0.53	1.72	0.000	0.006
Downregulated Gene Sets in MCF7-AR vs MCF7					
MSigDB HALLMARK	**SIZE**	**ES**	**NES**	**NOM p-val**	**FDR q-val**
HALLMARK_G2M_CHECKPOINT	190	-0.49	-1.86	0.000	0.002
HALLMARK_MYC_TARGETS_V1	194	-0.48	-1.81	0.000	0.003
HALLMARK_TGF_BETA_SIGNALING	50	-0.57	-1.74	0.002	0.008
HALLMARK_E2F_TARGETS	195	-0.45	-1.70	0.000	0.010
HALLMARK_ESTROGEN_RESPONSE_EARLY	193	-0.43	-1.64	0.000	0.015
HALLMARK_MITOTIC_SPINDLE	196	-0.41	-1.57	0.003	0.023
HALLMARK_IL2_STAT5_SIGNALING	142	-0.41	-1.49	0.004	0.044
Upregulated Gene Sets in MCF7-PR vs MCF7					
MSigDB HALLMARK	**SIZE**	**ES**	**NES**	**NOM p-val**	**FDR q-val**
HALLMARK_INTERFERON_ALPHA_RESPONSE	87	0.88	3.24	0.000	0.000
HALLMARK_INTERFERON_GAMMA_RESPONSE	155	0.80	3.20	0.000	0.000
HALLMARK_E2F_TARGETS	195	0.52	2.14	0.000	0.000
HALLMARK_G2M_CHECKPOINT	190	0.42	1.72	0.000	0.008
HALLMARK_MTORC1_SIGNALING	189	0.41	1.70	0.000	0.008
HALLMARK_CHOLESTEROL_HOMEOSTASIS	69	0.44	1.54	0.009	0.025
HALLMARK_ALLOGRAFT_REJECTION	97	0.41	1.53	0.010	0.025
HALLMARK_INFLAMMATORY_RESPONSE	111	0.40	1.55	0.003	0.027
HALLMARK_HEME_METABOLISM	153	0.39	1.56	0.002	0.029
Downregulated Gene Sets in MCF7-PR vs MCF7					
MSigDB HALLMARK	**SIZE**	**ES**	**NES**	**NOM p-val**	**FDR q-val**
HALLMARK_ESTROGEN_RESPONSE_EARLY	193	-0.61	-2.48	0.000	0.000
HALLMARK_ESTROGEN_RESPONSE_LATE	190	-0.56	-2.29	0.000	0.000
HALLMARK_EPITHELIAL_MESENCHYMAL_TRANSITION	136	-0.51	-2.00	0.000	0.000
HALLMARK_ANGIOGENESIS	26	-0.63	-1.81	0.003	0.001
HALLMARK_HYPOXIA	160	-0.41	-1.63	0.000	0.012
HALLMARK_MYOGENESIS	131	-0.40	-1.55	0.004	0.025
HALLMARK_UV_RESPONSE_DN	123	-0.39	-1.51	0.004	0.026
HALLMARK_COAGULATION	78	-0.42	-1.52	0.010	0.028
HALLMARK_APICAL_JUNCTION	143	-0.37	-1.47	0.005	0.036
Upregulated Gene Sets in T47D-AR vs T47D					
MSigDB HALLMARK	**SIZE**	**ES**	**NES**	**NOM p-val**	**FDR q-val**
HALLMARK_INTERFERON_ALPHA_RESPONSE	87	0.75	2.48	0.000	0.000
HALLMARK_INTERFERON_GAMMA_RESPONSE	155	0.62	2.19	0.000	0.000
HALLMARK_NOTCH_SIGNALING	29	0.71	1.91	0.000	0.000

HALLMARK_KRAS_SIGNALING_DN	100	0.55	1.88	0.000	0.000
HALLMARK_ANGIOGENESIS	26	0.62	1.65	0.009	0.012
HALLMARK_TNFA_SIGNALING_VIA_NFKB	163	0.44	1.56	0.000	0.022
HALLMARK_ESTROGEN_RESPONSE_EARLY	193	0.43	1.57	0.001	0.025
HALLMARK_ANDROGEN_RESPONSE	94	0.46	1.53	0.006	0.028
HALLMARK_HYPOXIA	160	0.42	1.51	0.002	0.034
HALLMARK_EPITHELIAL_MESENCHYMAL_TRANSITION	136	0.42	1.48	0.007	0.039
Downregulated Gene Sets in T47D-AR vs T47D					
MSigDB HALLMARK	**SIZE**	**ES**	**NES**	**NOM p-val**	**FDR q-val**
HALLMARK_E2F_TARGETS	195	-0.54	-2.14	0.000	0.000
HALLMARK_G2M_CHECKPOINT	190	-0.44	-1.74	0.000	0.004
HALLMARK_MYC_TARGETS_V1	194	-0.39	-1.55	0.000	0.034
Upregulated Gene Sets in T47D-PR vs T47D					
MSigDB HALLMARK	**SIZE**	**ES**	**NES**	**NOM p-val**	**FDR q-val**
HALLMARK_INTERFERON_ALPHA_RESPONSE	87	0.67	2.32	0.000	0.000
HALLMARK_INTERFERON_GAMMA_RESPONSE	155	0.62	2.31	0.000	0.000
HALLMARK_MYC_TARGETS_V2	58	0.54	1.73	0.002	0.007
HALLMARK_EPITHELIAL_MESENCHYMAL_TRANSITION	136	0.46	1.69	0.000	0.010
HALLMARK_ALLOGRAFT_REJECTION	97	0.44	1.52	0.005	0.045
HALLMARK_TNFA_SIGNALING_VIA_NFKB	163	0.40	1.49	0.006	0.051
Upregulated Gene Sets in T47D-PR vs T47D					
MSigDB HALLMARK	**SIZE**	**ES**	**NES**	**NOM p-val**	**FDR q-val**
HALLMARK_ESTROGEN_RESPONSE_EARLY	193	-0.57	-2.02	0.000	0.000
HALLMARK_ESTROGEN_RESPONSE_LATE	190	-0.57	-2.02	0.000	0.000
HALLMARK_BILE_ACID_METABOLISM	79	-0.52	-1.64	0.001	0.013

Supplementary Table S3 MSigDB Reactome gene sets significantly up- and downregulated in CDK4/6i resistant cell lines.

Upregulated Gene Sets in MCF7-AR vs MCF7					
MSigDB Reactome	**SIZE**	**ES**	**NES**	**NOM p-val**	**FDR q-val**
REACTOME_INTERFERON_ALPHA_BETA_SIGNALING	56	0.88	2.79	0.000	0.000
REACTOME_INTERFERON_SIGNALING	160	0.67	2.44	0.000	0.000
REACTOME_INTERFERON_GAMMA_SIGNALING	67	0.70	2.29	0.000	0.000
REACTOME_ANTIGEN_PRESENTATION_FOLDING_ASSEMBLY_AND_PEPTIDE_LOADING_OF_CLASS_I_MHC	25	0.77	2.06	0.000	0.001
REACTOME_IMMUNOREGULATORY_INTERACTIONS_BETWEEN_A_LYMPHOID_AND_A_NON_LYMPHOID_CELL	41	0.63	1.88	0.000	0.017
REACTOME_ANTIVIRAL_MECHANISM_BY_IFN_STIMULATED_GENES	79	0.56	1.86	0.000	0.021
REACTOME_NICOTINATE_METABOLISM	19	0.72	1.81	0.002	0.038
Downregulated Gene Sets in MCF7-AR vs MCF7					
MSigDB Reactome	**SIZE**	**ES**	**NES**	**NOM p-val**	**FDR q-val**
REACTOME_TRANSPORT_OF_MATURE_MRNAS_DERIVED_FROM_INTRONLESS_TRANSCRIPTS	41	-0.69	-2.08	0.000	0.002
REACTOME_SUMOYLATION_OF_DNA_REPLICATION_PROTEINS	44	-0.67	-2.00	0.000	0.003
REACTOME_TRANSPORT_OF_THE_SLBP_DEPENDANT_MATURE_MRNA	34	-0.71	-2.03	0.000	0.004
REACTOME_NUCLEAR_IMPORT_OF_REV_PROTEIN	32	-0.71	-2.03	0.000	0.004
REACTOME_INTERACTIONS_OF_REV_WITH_HOST_CELLULAR_PROTEINS	35	-0.68	-1.98	0.000	0.006
REACTOME_REGULATION_OF_GLUCOKINASE_BY_GLUCOKINASE_REGULATORY_PROTEIN	28	-0.71	-1.97	0.003	0.006
REACTOME_SUMOYLATION_OF_SUMOYLATION_PROTEINS	33	-0.69	-1.94	0.000	0.007
REACTOME_SIGNALING_BY_TGFB_FAMILY_MEMBERS	92	-0.56	-1.93	0.000	0.007
REACTOME_NUCLEAR_PORE_COMPLEX_NPC_DISASSEMBLY	34	-0.66	-1.91	0.000	0.010
REACTOME_TRANSCRIPTIONAL_REGULATION_BY_SMALL_RNAS	45	-0.62	-1.87	0.000	0.015
REACTOME_EXPORT_OF_VIRAL_RIBONUCLEOPROTEINS_FROM_NUCLEUS	31	-0.67	-1.86	0.000	0.016
REACTOME_GLYCOGEN_METABOLISM	24	-0.69	-1.85	0.001	0.016
REACTOME_CHROMATIN_MODIFYING_ENZYMES	187	-0.49	-1.87	0.000	0.016
REACTOME_SIGNALING_BY_BMP	20	-0.73	-1.86	0.000	0.016
REACTOME_RRNA_MODIFICATION_IN_THE_NUCLEUS_AND_CYTOSOL	54	-0.58	-1.88	0.000	0.016
REACTOME_SIGNALING_BY_TGF_BETA_RECEPTOR_COMPLEX	72	-0.56	-1.85	0.000	0.017
REACTOME_TP53_REGULATES_TRANSCRIPTION_OF_CELL_CYCLE_GENES	46	-0.61	-1.83	0.001	0.020
REACTOME_TRANSCRIPTIONAL_ACTIVITY_OF_SMAD2_SMAD3_SMAD4_HETEROTRIMER	43	-0.61	-1.82	0.001	0.020
REACTOME_HCMV_LATE_EVENTS	51	-0.59	-1.83	0.002	0.020

REACTOME_SMAD2_SMAD3_SMAD4_HETEROTRIMER_REGULATES_TRANSCRIPTION	31	-0.65	-1.83	0.001	0.021
REACTOME_INTERACTIONS_OF_VPR_WITH_HOST_CELLULAR_PROTEINS	35	-0.63	-1.81	0.003	0.022
REACTOME_PROCESSING_OF_CAPPED_INTRON_CONTAINING_PRE_MRNA	232	-0.47	-1.81	0.000	0.023
REACTOME_POSTMITOTIC_NUCLEAR_PORE_COMPLEX_NPC_REFORMATION	26	-0.66	-1.80	0.001	0.024
REACTOME_E2F_MEDIATED_REGULATION_OF_DNA_REPLICATION	22	-0.68	-1.79	0.003	0.024
REACTOME_VIRAL_MESSENGER_RNA_SYNTHESIS	42	-0.61	-1.81	0.000	0.024
REACTOME_GENE_SILENCING_BY_RNA	66	-0.55	-1.80	0.000	0.025
REACTOME_SUMOYLATION_OF_RNA_BINDING_PROTEINS	45	-0.59	-1.79	0.004	0.025
REACTOME_SNRNP_ASSEMBLY	52	-0.57	-1.78	0.001	0.026
REACTOME_ACTIVATION_OF_BH3_ONLY_PROTEINS	29	-0.63	-1.78	0.002	0.026
REACTOME_RMTS_METHYLATE_HISTONE_ARGININES	29	-0.64	-1.77	0.001	0.027
REACTOME_EPIGENETIC_REGULATION_OF_GENE_EXPRESSION	83	-0.53	-1.77	0.000	0.027
REACTOME_TRANSCRIPTION_OF_E2F_TARGETS_UNDER_NEGATIVE_CONTROL_BY_P107_RBL1_AND_P130_RBL2_IN_COMPLEX_WITH_HDAC1	16	-0.71	-1.76	0.006	0.030
REACTOME_RND2_GTPASE_CYCLE	39	-0.60	-1.75	0.001	0.032
REACTOME_G1_S_SPECIFIC_TRANSCRIPTION	28	-0.64	-1.75	0.003	0.036
REACTOME_SUMOYLATION_OF_UBIQUITINYLATION_PROTEINS	37	-0.59	-1.74	0.001	0.038
REACTOME_SUMOYLATION_OF_CHROMATIN_ORGANIZATION_PROTEINS	55	-0.54	-1.73	0.001	0.042
REACTOME_TP53_REGULATES_TRANSCRIPTION_OF_GENES_INVOLVED_IN_CYTOCHROME_C_RELEASE	18	-0.69	-1.73	0.004	0.042
REACTOME_G0_AND_EARLY_G1	26	-0.64	-1.72	0.006	0.045
REACTOME_TRANSPORT_OF_MATURE_TRANSCRIPT_TO_CYTOPLASM	79	-0.51	-1.72	0.000	0.045
REACTOME_DEADENYLATION_DEPENDENT_MRNA_DECAY	53	-0.54	-1.71	0.002	0.049
Upregulated Gene Sets in MCF7-PR vs MCF7					
MSigDB Reactome	**SIZE**	**ES**	**NES**	**NOM p-val**	**FDR q-val**
REACTOME_INTERFERON_ALPHA_BETA_SIGNALING	56	0.86	2.94	0.000	0.000
REACTOME_INTERFERON_SIGNALING	160	0.65	2.60	0.000	0.000
REACTOME_ANTIVIRAL_MECHANISM_BY_IFN_STIMULATED_GENES	79	0.62	2.22	0.000	0.000
REACTOME_INTERFERON_GAMMA_SIGNALING	67	0.61	2.15	0.000	0.000
REACTOME_ANTIGEN_PRESENTATION_FOLDING_ASSEMBLY_AND_PEPTIDE_LOADING_OF_CLASS_I_MHC	25	0.73	2.08	0.000	0.001
REACTOME_NICOTINATE_METABOLISM	19	0.76	2.05	0.000	0.001
REACTOME_CELL_CYCLE_CHECKPOINTS	243	0.48	2.03	0.000	0.001
REACTOME_MITOTIC_SPINDLE_CHECKPOINT	105	0.52	1.98	0.000	0.004
REACTOME_NEGATIVE_REGULATORS_OF_DDX58_IFIH1_SIGNALING	34	0.65	1.98	0.000	0.004

REACTOME_HOMOLOGOUS_DNA_PAIRING_AND_STRAND_EXCHANGE	41	0.61	1.98	0.000	0.004
REACTOME_NONHOMOLOGOUS_END_JOINING_NHEJ	30	0.66	1.98	0.000	0.004
REACTOME_ACTIVATION_OF_ATR_IN_RESPONSE_TO_REPLICATION_STRESS	37	0.62	1.93	0.000	0.007
REACTOME_TRANSLATION_OF_SARS_COV_1_STRUCTURAL_PROTEINS	27	0.66	1.93	0.000	0.007
REACTOME_METABOLISM_OF_PORPHYRINS	18	0.71	1.90	0.001	0.011
REACTOME_TRANSLATION_OF_SARS_COV_2_STRUCTURAL_PROTEINS	42	0.59	1.88	0.000	0.014
REACTOME_DDX58_IFIH1_MEDIATED_INDUCTION_OF_INTERFERON_ALPHA_BETA	61	0.54	1.87	0.000	0.015
REACTOME_METABOLISM_OF_WATER_SOLUBLE_VITAMINS_AND_COFACTORS	91	0.49	1.85	0.000	0.017
REACTOME_ANTIGEN_PROCESSING_CROSS_PRESENTATION	88	0.50	1.85	0.000	0.017
REACTOME_HDR_THROUGH_HOMOLOGOUS_RECOMBINATION_HRR	65	0.52	1.84	0.001	0.018
REACTOME_G2_M_DNA_DAMAGE_CHECKPOINT	57	0.54	1.83	0.000	0.019
REACTOME_PROCESSING_OF_DNA_DOUBLE_STRAND_BREAK_ENDS	59	0.53	1.83	0.001	0.019
REACTOME_CYTOKINE_SIGNALING_IN_IMMUNE_SYSTEM	492	0.40	1.82	0.000	0.019
REACTOME_DNA_DOUBLE_STRAND_BREAK_REPAIR	125	0.47	1.81	0.000	0.022
REACTOME_TERMINATION_OF_TRANSLESION_DNA_SYNTHESIS	31	0.60	1.80	0.001	0.022
REACTOME_ACTIVATION_OF_THE_PRE_REPLICATIVE_COMPLEX	32	0.59	1.79	0.000	0.024
REACTOME_DNA_DAMAGE_BYPASS	46	0.55	1.79	0.000	0.024
REACTOME_HOMOLOGY_DIRECTED_REPAIR	98	0.48	1.79	0.000	0.025
REACTOME_MITOTIC_PROMETAPHASE	184	0.43	1.78	0.000	0.025
REACTOME_TRANSLESION_SYNTHESIS_BY_Y_FAMILY_DNA_POLYMERASES_BYPASSES_LESIONS_ON_DNA_TEMPLATE	37	0.56	1.78	0.001	0.026
REACTOME_NUCLEOBASE_CATABOLISM	27	0.61	1.77	0.002	0.027
REACTOME_G2_M_CHECKPOINTS	127	0.45	1.77	0.000	0.027
REACTOME_HDR_THROUGH_SINGLE_STRAND_ANNEALING_SSA	36	0.57	1.76	0.004	0.029
REACTOME_RESPONSE_OF_EIF2AK1_HRI_TO_HEME_DEFICIENCY	15	0.69	1.74	0.007	0.034
REACTOME_RESOLUTION_OF_D_LOOP_STRUCTURES_THROUGH_SYNTHESIS_DEPENDENT_STRAND_ANNEALING_SDSA	25	0.60	1.73	0.003	0.038
Downregulated Gene Sets in MCF7-PR vs MCF7					
MSigDB Reactome	**SIZE**	**ES**	**NES**	**NOM p-val**	**FDR q-val**
REACTOME_SEMAPHORIN_INTERACTIONS	53	-0.65	-2.20	0.000	0.000
REACTOME_EUKARYOTIC_TRANSLATION_ELONGATION	89	-0.58	-2.14	0.000	0.001
REACTOME_KERATINIZATION	39	-0.61	-1.97	0.000	0.012
REACTOME_GAP_JUNCTION_ASSEMBLY	17	-0.75	-1.97	0.001	0.014
REACTOME_EUKARYOTIC_TRANSLATION_INITIATION	116	-0.51	-1.98	0.000	0.016

REACTOME_FORMATION_OF_THE_CORNIFIED_ENVELOPE	39	-0.61	-1.93	0.000	0.017
REACTOME_GAP_JUNCTION_TRAFFICKING_AND_REGULATION	30	-0.64	-1.91	0.000	0.020
REACTOME_POST_CHAPERONIN_TUBULIN_FOLDING_PATHWAY	15	-0.75	-1.88	0.002	0.031
REACTOME_NONSENSE_MEDIATED_DECAY_NMD	112	-0.49	-1.87	0.000	0.032
REACTOME_NERVOUS_SYSTEM_DEVELOPMENT	471	-0.41	-1.86	0.000	0.033
REACTOME_O_GLYCOSYLATION_OF_TSR_DOMAIN_CONTAINING_PROTEINS	20	-0.67	-1.84	0.001	0.039
Upregulated Gene Sets in T47D-AR vs T47D					
MSigDB Reactome	**SIZE**	**ES**	**NES**	**NOM p-val**	**FDR q-val**
REACTOME_INTERFERON_ALPHA_BETA_SIGNALING	56	0.76	2.34	0.000	0.000
REACTOME_INTERFERON_GAMMA_SIGNALING	67	0.62	1.96	0.000	0.009
REACTOME_INTERFERON_SIGNALING	160	0.53	1.91	0.000	0.018
REACTOME_NON_INTEGRIN_MEMBRANE_ECM_INTERACTIONS	44	0.63	1.88	0.000	0.024
REACTOME_HS_GAG_DEGRADATION	21	0.71	1.83	0.003	0.032
REACTOME_IRE1ALPHA_ACTIVATES_CHAPERONES	46	0.61	1.82	0.001	0.033
REACTOME_COLLAGEN_CHAIN_TRIMERIZATION	22	0.70	1.81	0.002	0.035
REACTOME_COLLAGEN_DEGRADATION	34	0.65	1.84	0.003	0.036
Downregulated Gene Sets in T47D-AR vs T47D					
MSigDB Reactome	**SIZE**	**ES**	**NES**	**NOM p-val**	**FDR q-val**
REACTOME_EUKARYOTIC_TRANSLATION_ELONGATION	89	-0.52	-1.85	0.000	0.040
REACTOME_NUCLEAR_PORE_COMPLEX_NPC_DISASSEMBLY	34	-0.62	-1.85	0.000	0.042
REACTOME_CHROMOSOME_MAINTENANCE	85	-0.53	-1.89	0.000	0.042
REACTOME_ACTIVATION_OF_THE_PRE_REPLICATIVE_COMPLEX	32	-0.61	-1.80	0.000	0.042
REACTOME_RNA_POLYMERASE_II_TRANSCRIPTION_TERMINATION	65	-0.54	-1.82	0.001	0.042
REACTOME_PROCESSING_OF_CAPPED_INTRON_CONTAINING_PRE_MRNA	232	-0.45	-1.83	0.000	0.043
REACTOME_MITOTIC_PROMETAPHASE	184	-0.47	-1.86	0.000	0.044
REACTOME_HOMOLOGOUS_DNA_PAIRING_AND_STRAND_EXCHANGE	41	-0.59	-1.82	0.001	0.045
REACTOME_EUKARYOTIC_TRANSLATION_INITIATION	116	-0.49	-1.80	0.000	0.045
REACTOME_SUMOYLATION_OF_CHROMATIN_ORGANIZATION_PROTEINS	55	-0.56	-1.81	0.000	0.045
REACTOME_ACTIVATION_OF_ATR_IN_RESPONSE_TO_REPLICATION_STRESS	37	-0.60	-1.80	0.002	0.045
REACTOME_NUCLEAR_ENVELOPE_BREAKDOWN	50	-0.56	-1.79	0.001	0.046
REACTOME_DEPOSITION_OF_NEW_CENPA_CONTAINING_NUCLEOSOMES_AT_THE_CENTROMERE	24	-0.64	-1.77	0.003	0.047
REACTOME_DNA_STRAND_ELONGATION	32	-0.61	-1.78	0.000	0.048

REACTOME_TRANSPORT_OF_THE_SLBP_DEPENDANT_MATURE_MRNA	34	-0.58	-1.75	0.005	0.048
REACTOME_CHOLESTEROL_BIOSYNTHESIS	23	-0.69	-1.87	0.000	0.048
REACTOME_AURKA_ACTIVATION_BY_TPX2	68	-0.51	-1.75	0.000	0.049
REACTOME_RESOLUTION_OF_D_LOOP_STRUCTURES_THROUGH_SYNTHESIS_DEPENDENT_STRAND_ANNEALING_SDSA	25	-0.64	-1.77	0.004	0.049
REACTOME_TRANSCRIPTION_OF_E2F_TARGETS_UNDER_NEGATIVE_CONTROL_BY_DREAM_COMPLEX	19	-0.67	-1.75	0.004	0.049
REACTOME_TRANSPORT_OF_MATURE_TRANSCRIPT_TO_CYTOPLASM	79	-0.55	-1.92	0.000	0.050
REACTOME_ACTIVATION_OF_ANTERIOR_HOX_GENES_IN_HINDBRAIN_DEVELOPMENT_DURING_EARLY_EMBRYOGENESIS	51	-0.54	-1.76	0.000	0.050
Upregulated Gene Sets in T47D-PR vs T47D					
Reactome	**SIZE**	**ES**	**NES**	**NOM p-val**	**FDR q-val**
REACTOME_INTERFERON_ALPHA_BETA_SIGNALING	56	0.82	2.57	0.000	0.000
REACTOME_INTERFERON_SIGNALING	160	0.56	2.06	0.000	0.004
REACTOME_IMMUNOREGULATORY_INTERACTIONS_BETWEEN_A_LYMPHOID_AND_A_NON_LYMPHOID_CELL	41	0.64	1.92	0.000	0.021
REACTOME_ANTIVIRAL_MECHANISM_BY_IFN_STIMULATED_GENES	79	0.57	1.93	0.000	0.025

Supplementary Table S4 RPPA data.

	MCF7-AR vs MCF7			MCF7-PR vs MCF7			T47D-AR vs T47D			T47D-PR vs T47D		
Antibody	**Ratio**	**Log2FC**	**p-value**	**Ratio**	**Log2FC**	**p-value**	**Ratio**	**Log2FC**	**p-value**	**Ratio**	**Log2FC**	**p-value**
4E-BP1 S65	0.33	-1.59	0.00003	0.97	-0.05	0.34262	0.50	-0.99	0.00007	0.78	-0.37	0.00012
4E-BP1 T70	1.01	0.02	0.77966	1.72	0.78	0.00012	0.91	-0.13	0.15426	1.02	0.03	0.68391
AKT S473	0.19	-2.39	0.00066	0.85	-0.24	0.14699	0.45	-1.15	0.00011	0.49	-1.02	0.00029
AKT S473 XP	0.20	-2.35	0.00133	0.77	-0.37	0.09389	0.44	-1.19	0.00003	0.55	-0.87	0.00250
AKT T308	0.38	-1.38	0.00237	0.89	-0.17	0.33383	0.60	-0.73	0.01559	0.94	-0.09	0.77501
AKT total	1.33	0.41	0.00964	0.84	-0.25	0.01277	1.10	0.13	0.05091	1.16	0.21	0.02419
ALK Y1586	0.78	-0.35	0.00115	0.99	-0.01	0.86989	0.88	-0.18	0.00046	1.01	0.02	0.75273
ALK Y1604	1.19	0.25	0.09408	0.85	-0.24	0.14058	1.02	0.02	0.82907	0.95	-0.08	0.76013
AMPK alpha T172	0.72	-0.47	0.02539	0.98	-0.04	0.78281	1.31	0.39	0.02701	1.42	0.50	0.04146
AMPK alpha1 S485	0.59	-0.75	0.00962	0.91	-0.13	0.53846	0.91	-0.14	0.24372	1.33	0.41	0.20481
Androgen Rec total	0.96	-0.05	0.72481	1.42	0.51	0.01616	1.27	0.34	0.09101	1.00	0.00	0.99925
ATM S1981	1.04	0.06	0.65309	0.88	-0.18	0.17555	0.80	-0.32	0.01345	0.90	-0.15	0.25946
AXL Y702	0.65	-0.61	0.40846	0.94	-0.09	0.86237	0.73	-0.45	0.12710	0.63	-0.66	0.40608
BAD S112	0.99	-0.02	0.88126	1.52	0.60	0.04190	0.75	-0.42	0.02966	0.93	-0.10	0.45048
BAD S136	0.98	-0.02	0.69475	1.44	0.53	0.00098	0.85	-0.23	0.00507	0.96	-0.06	0.71468
BAD total	3.11	1.64	0.00021	1.60	0.68	0.02030	1.07	0.10	0.49518	0.64	-0.64	0.00021
BCL-2 total	3.12	1.64	0.01963	1.54	0.62	0.00845	1.01	0.02	0.94208	0.75	-0.42	0.27128

BIM total	0.76	-0.40	0.02075	0.89	-0.17	0.24850	0.51	-0.96	0.00127	0.93	-0.11	0.19782
c-MYC S62	0.96	-0.06	0.66331	1.10	0.14	0.28777	0.29	-1.80	0.00001	0.74	-0.43	0.02038
c-MYC total	1.06	0.09	0.13858	1.13	0.18	0.05372	0.69	-0.53	0.00354	0.86	-0.22	0.06699
C-RAF S338	0.89	-0.17	0.09587	0.80	-0.32	0.00033	0.71	-0.50	0.00276	0.89	-0.16	0.19130
cABL T735	0.93	-0.10	0.45722	1.05	0.07	0.23414	0.80	-0.32	0.02592	0.93	-0.11	0.37723
Caspase 3 cleaved D175	0.99	-0.01	0.90898	1.00	0.00	0.97999	0.97	-0.05	0.28882	1.15	0.20	0.16319
Caspase 9 cleaved D330	1.08	0.11	0.30471	1.04	0.06	0.10741	0.99	-0.01	0.90585	0.98	-0.03	0.78708
cKIT Y703	1.11	0.14	0.19383	0.98	-0.02	0.35123	0.93	-0.10	0.13412	0.99	-0.02	0.87480
Collagen Type 1 total	1.50	0.59	0.48353	1.67	0.74	0.28452	1.18	0.24	0.71582	0.86	-0.22	0.82531
Cyclin D1 total	1.53	0.61	0.00288	1.23	0.30	0.00698	1.36	0.44	0.01590	0.98	-0.02	0.90667
EGFR total	0.94	-0.09	0.12282	1.48	0.57	0.00108	0.90	-0.15	0.30600	1.13	0.18	0.20708
EGFR Y1068	0.81	-0.30	0.07731	1.02	0.03	0.85500	0.35	-1.53	0.07165	1.57	0.65	0.10817
EGFR Y1173	0.91	-0.14	0.06027	0.93	-0.10	0.15636	0.93	-0.10	0.07552	1.04	0.06	0.44415
eIF2alpha S51	1.16	0.22	0.21389	0.95	-0.07	0.68348	1.04	0.05	0.68408	0.60	-0.73	0.03092
eIF4E S209	1.21	0.27	0.10439	0.86	-0.22	0.11396	1.25	0.32	0.00611	1.19	0.25	0.07130
eIF4G S1108	0.47	-1.10	0.00098	0.91	-0.14	0.22587	0.51	-0.98	0.00031	1.42	0.51	0.00239
ERK1/2 T202/Y204	1.16	0.22	0.03246	1.09	0.13	0.15779	1.03	0.05	0.68649	0.49	-1.02	0.00049
ERK1/2 total	1.25	0.32	0.00285	1.01	0.01	0.82965	0.93	-0.10	0.35713	0.78	-0.36	0.01121
Estrogen Rec alpha S118	0.98	-0.02	0.70819	0.97	-0.05	0.36925	0.89	-0.17	0.03868	0.83	-0.26	0.01248
Estrogen Rec alpha total	0.60	-0.74	0.00576	0.52	-0.95	0.00170	0.85	-0.23	0.54034	0.59	-0.77	0.09174

FGF Rec Y653/Y654	1.10	0.14	0.04697	0.95	-0.07	0.20918	0.89	-0.18	0.02383	0.97	-0.04	0.65992
Fibronectin total	1.11	0.15	0.08833	1.05	0.07	0.34687	0.96	-0.06	0.07860	0.84	-0.24	0.01541
FOXM1 T600	0.80	-0.33	0.13902	0.93	-0.10	0.57205	0.62	-0.69	0.01308	0.72	-0.48	0.08712
FOXO1 S256	0.73	-0.45	0.02942	1.02	0.02	0.87082	0.66	-0.61	0.00575	0.90	-0.16	0.39437
FOXO1 T24/FOXO3 T32	0.35	-1.50	0.00017	0.93	-0.11	0.18487	0.81	-0.31	0.04045	0.88	-0.18	0.35215
GAPDH total	1.37	0.46	0.04105	1.27	0.34	0.03746	0.98	-0.04	0.83593	0.90	-0.16	0.19971
GSK3aB S21/S9	0.29	-1.79	0.00151	0.60	-0.74	0.01208	0.92	-0.11	0.67422	1.48	0.56	0.19135
GSK3aB Y279/Y216	0.49	-1.04	0.00057	0.83	-0.26	0.04189	0.50	-1.00	0.00011	0.89	-0.17	0.11039
HER2 total	1.04	0.06	0.70877	1.20	0.27	0.16019	0.40	-1.34	0.00136	0.75	-0.41	0.09933
HER2 Y1248	1.20	0.27	0.01086	1.00	0.00	0.96786	0.68	-0.55	0.00205	0.79	-0.34	0.06950
HER2 Y877	0.96	-0.06	0.26056	0.98	-0.03	0.35411	1.03	0.04	0.26024	1.00	0.00	0.94469
HER3 total	1.38	0.46	0.06264	1.18	0.23	0.07229	0.68	-0.56	0.01906	1.04	0.06	0.73519
HER3 Y1197	1.13	0.17	0.20785	1.41	0.50	0.01393	0.69	-0.53	0.00247	0.72	-0.47	0.01148
HER3 Y1289	0.68	-0.55	0.00266	0.69	-0.55	0.00391	0.71	-0.50	0.00053	0.73	-0.46	0.00107
HSP70 total	2.52	1.33	0.04348	1.58	0.66	0.01837	1.18	0.24	0.68088	0.57	-0.81	0.31285
HSP90 total	1.43	0.52	0.25267	1.12	0.16	0.25684	0.45	-1.16	0.01869	0.59	-0.75	0.07974
HSP90a T5/T7	1.00	0.00	0.97121	0.88	-0.18	0.11480	0.90	-0.15	0.13118	1.04	0.05	0.81741
IGF-1 Rec Y1131/Insulin Rec Y1146	0.98	-0.03	0.67927	0.78	-0.36	0.00923	0.92	-0.11	0.31234	1.06	0.08	0.46878

IGF-1 Rec Y1135/Y1136_Insulin Rec Y1150/Y1151	1.09	0.12	0.40515	1.01	0.02	0.88573	0.84	-0.25	0.21109	0.88	-0.18	0.59930
IL-6 total	1.08	0.11	0.01349	0.87	-0.20	0.00727	0.86	-0.22	0.18851	0.84	-0.25	0.07954
Insulin Rec beta total	1.28	0.36	0.00922	1.13	0.18	0.00559	0.93	-0.11	0.15725	1.29	0.37	0.01790
IRS1 S612	0.99	-0.01	0.81704	0.89	-0.17	0.08006	0.91	-0.14	0.21900	0.89	-0.17	0.16900
IRS1 total	0.95	-0.07	0.56249	1.02	0.03	0.80519	1.52	0.60	0.00222	0.67	-0.59	0.00508
JAK2 Y1007	0.89	-0.17	0.32388	0.80	-0.32	0.03428	0.77	-0.39	0.06675	0.92	-0.13	0.39644
Ki67 total	0.68	-0.55	0.00716	1.60	0.68	0.00012	0.14	-2.80	0.00012	0.33	-1.58	0.00044
LKB1 S334	1.06	0.09	0.04584	0.94	-0.09	0.04858	0.96	-0.05	0.20346	1.06	0.08	0.76889
M-CSF Rec Y723	1.37	0.46	0.05005	1.07	0.09	0.28849	0.77	-0.37	0.03328	0.89	-0.17	0.34803
MEK1/2 S217/S221	0.97	-0.05	0.83721	0.98	-0.04	0.77578	0.68	-0.55	0.00358	0.86	-0.22	0.24621
MET Y1234/Y1235	1.27	0.35	0.00222	0.91	-0.13	0.00742	0.90	-0.15	0.05171	0.93	-0.11	0.10100
MLH1 total	1.13	0.18	0.23385	1.21	0.27	0.08944	0.54	-0.89	0.00049	0.60	-0.75	0.00047
mTOR S2448	1.09	0.13	0.53115	1.00	0.01	0.95599	0.70	-0.52	0.00996	0.97	-0.04	0.82280
NFkB p65 S536	0.93	-0.11	0.58030	1.12	0.17	0.23688	1.15	0.20	0.27384	1.07	0.09	0.88623
NPM T199	0.77	-0.37	0.09884	0.87	-0.20	0.35024	1.04	0.05	0.42066	1.18	0.24	0.26356
p27 T187	0.45	-1.17	0.00038	0.75	-0.42	0.01051	0.66	-0.60	0.00508	0.83	-0.28	0.11651
p38 MAPK T180/Y182	0.84	-0.25	0.28014	0.89	-0.16	0.41227	1.00	0.00	0.99080	1.31	0.39	0.15654
p70S6K S371	1.13	0.17	0.04966	1.09	0.12	0.04045	1.03	0.04	0.52666	1.03	0.05	0.67946

p70S6K T389	0.61	-0.71	0.00581	0.59	-0.76	0.00482	1.33	0.41	0.03306	1.81	0.85	0.00772
p70S6K T412	0.59	-0.77	0.00046	0.64	-0.66	0.00183	1.32	0.40	0.02972	1.85	0.89	0.01319
p90RSK S380	0.87	-0.20	0.32390	1.02	0.03	0.84619	0.22	-2.21	0.24327	N/A	N/A	N/A
p90RSK T359/S363	0.61	-0.71	0.10241	0.89	-0.17	0.52217	0.75	-0.42	0.08537	0.63	-0.66	0.15557
PARP cleaved D214	2.96	1.57	0.00161	1.34	0.43	0.02593	1.32	0.40	0.06493	1.24	0.32	0.07906
PD-1 total (Nivolumab)	1.26	0.33	0.16980	1.07	0.09	0.35084	0.77	-0.38	0.05607	0.90	-0.15	0.52470
PD-1 total (Pembrolizumab)	1.25	0.32	0.15757	0.98	-0.02	0.80810	0.71	-0.49	0.02611	0.83	-0.26	0.23257
PD-L1 total (28-8)	1.27	0.34	0.06442	1.02	0.03	0.64685	0.89	-0.17	0.10720	0.87	-0.19	0.32399
PD-L1 total (Atezolizumab)	1.44	0.52	0.04752	0.88	-0.18	0.02005	0.83	-0.28	0.04410	0.88	-0.18	0.25831
PD-L1 total (SP142)	1.15	0.20	0.13370	1.07	0.09	0.50518	1.26	0.33	0.02767	1.26	0.33	0.54309
PDGF Rec beta Y716	1.28	0.35	0.01210	0.92	-0.12	0.02709	1.04	0.05	0.29736	0.99	-0.01	0.93691
PDGF Rec beta Y751	1.28	0.36	0.18432	1.35	0.44	0.11346	1.57	0.65	0.00052	1.28	0.36	0.11265
PI3K p85 Y458_p55 Y199	1.12	0.17	0.28377	1.09	0.12	0.17845	1.00	0.00	0.97021	1.21	0.27	0.13285
PRAS40 T246	0.13	-2.92	0.00013	0.54	-0.88	0.00208	0.61	-0.72	0.00147	1.39	0.48	0.04661
PTEN S380	1.17	0.22	0.35196	0.75	-0.42	0.00367	0.79	-0.34	0.05065	1.12	0.17	0.45326
PTEN total	1.23	0.30	0.08461	0.78	-0.37	0.04722	1.14	0.18	0.00487	1.11	0.15	0.06493
RB S780	0.68	-0.55	0.00082	0.71	-0.49	0.00032	0.75	-0.41	0.01699	0.74	-0.44	0.01977
RET Y905	1.31	0.38	0.02913	0.67	-0.58	0.00405	0.81	-0.31	0.00131	1.05	0.07	0.71711
RON Y1353	0.81	-0.31	0.07040	1.09	0.12	0.31256	1.31	0.39	0.01480	1.14	0.19	0.17881

S6RP S240/S244	0.51	-0.96	0.00042	0.96	-0.06	0.68011	0.64	-0.65	0.00576	1.71	0.77	0.00142
SGK1 S78	1.31	0.39	0.07076	0.87	-0.20	0.02462	0.74	-0.44	0.01006	0.90	-0.15	0.45128
SRC Family Y416	0.82	-0.29	0.02730	0.72	-0.47	0.00164	0.81	-0.31	0.23161	1.21	0.27	0.63741
SRC Y527	0.60	-0.73	0.00600	0.58	-0.79	0.00427	0.86	-0.22	0.04094	0.74	-0.43	0.00352
STAT1 S727	1.55	0.63	0.00615	2.68	1.42	0.00018	2.17	1.12	0.00008	2.15	1.10	0.01036
STAT1 Y701	1.07	0.10	0.72477	1.53	0.62	0.03638	1.25	0.33	0.06227	0.92	-0.13	0.68494
STAT3 S727	1.44	0.52	0.08343	1.35	0.43	0.01192	1.59	0.67	0.00536	1.80	0.85	0.02668
STAT3 Y705	2.05	1.03	0.00502	1.11	0.15	0.11079	1.02	0.03	0.80366	1.03	0.04	0.87267
STAT4 Y693	1.02	0.03	0.72041	1.06	0.08	0.24995	1.02	0.03	0.62282	1.00	0.00	0.99064
STAT5 Y694	0.31	-1.67	0.00010	0.39	-1.35	0.00011	0.71	-0.50	0.00428	0.66	-0.60	0.02163
STAT6 Y641	0.51	-0.99	0.00074	0.55	-0.88	0.00069	1.00	-0.01	0.85384	0.88	-0.18	0.44132
Tuberin/TSC2 Y1571	1.19	0.25	0.07327	0.93	-0.11	0.19405	0.84	-0.25	0.00703	0.88	-0.18	0.16295
YAP S127	1.13	0.18	0.14728	0.97	-0.04	0.58386	1.39	0.48	0.01042	1.49	0.58	0.00091

Supplementary Table S5 Immunoblot Antibodies.

Antibody	Dilution	Product Number	Source
HER3 total	1:1000	4754	Cell Signaling Technology
HER3 Y1289	1:500	4791	Cell Signaling Technology
HER2 total	1:1000	2242	Cell Signaling Technology
HER2 Y1221/1222	1:1000	2249	Cell Signaling Technology
EGFR total	1:1000	4267	Cell Signaling Technology
EGFR Y1068	1:500	3777	Cell Signaling Technology
STAT1 total	1:3000	14994	Cell Signaling Technology
STAT1 Y701	1:1000	7649	Cell Signaling Technology
STAT1 S727	1:2000	8826	Cell Signaling Technology
PR	1:500	8757	Cell Signaling Technology
ER	1:1000	8644	Cell Signaling Technology
pan-AKT	1:3000	4691	Cell Signaling Technology
AKT S473	1:1000	4060	Cell Signaling Technology
Rb total	1:2000	9309	Cell Signaling Technology
Rb S807/S811	1:1000	8516	Cell Signaling Technology
Cyclin D1	1:50,000	ab134175	Abcam
Cyclin E	1:1000	sc-247	Santa Cruz
Cyclin E2	1:500	4132	Cell Signaling Technology
CDK4	1:1000	12790	Cell Signaling Technology
CDK6	1:1000	sc-7961	Santa Cruz
70S6K total	1:1000	2708	Cell Signaling Technology
70S6K T389	1:1000	9205	Cell Signaling Technology
S6RP total	1:3000	2217	Cell Signaling Technology
S6RP S240/244	1:3000	5364	Cell Signaling Technology
4E-BP1 total	1:3000	9644	Cell Signaling Technology
4E-BP1 S65	1:3000	13443	Cell Signaling Technology
β-actin (IgM)	1:100,000	60008-I-Ig	Proteintech
α-Rabbit IgG HRP-linked	1:2000	7074	Cell Signaling Technology
α-Mouse IgG HRP-linked	1:2000	7076	Cell Signaling Technology
α-Mouse IgM HRP-linked	1:25,000	401225	EMD Millipore

Supplementary Table S6 Taqman Primers.

Target Gene	TaqMan Assay
CCND1	Hs00765553_m1
CCNE1	Hs01026536_m1
CCNE2	Hs00180319_m1
CDK4	Hs00364847_m1
CDK6	Hs01026371_m1
CDKN2A	Hs00923894_m1
EGFR	Hs01076090_m1
ERBB2	Hs01001580_m1
ERBB3	Hs00176538_m1
ERBB4	Hs00171783_m1
ESR1	Hs00174860_m1
IFI44	Hs00197427_m1
IFI6	Hs00242571_m1
IFIT1	Hs03027069_s1
MX1	Hs00895608_m1
OAS1	Hs00973635_m1
OAS2	Hs00942643_m1
PGR	Hs01556702_m1
RB1	Hs01078066_m1
RPL37A	Hs01102345_m1
STAT1	Hs01013996_m1

Supplementary Table S7 RPPA Antibodies.

Antibody	Array Dilution	Product Number	Source
4E-BP1 S65	1:50	9451	Cell Signaling Technology
4E-BP1 T70	1:200	9455	Cell Signaling Technology
AKT S473	1:100	9271	Cell Signaling Technology
AKT S473 XP	1:100	4060	Cell Signaling Technology
AKT T308	1:100	9275	Cell Signaling Technology
AKT total	1:2000	9272	Cell Signaling Technology
ALK Y1586	1:200	3348	Cell Signaling Technology
ALK Y1604	1:50	3341	Cell Signaling Technology
AMPK alpha T172	1:2000	4188	Cell Signaling Technology
AMPK alpha1 S485	1:50	4184	Cell Signaling Technology
Androgen Rec total	1:100	M3562	Dako/Agilent
ATM S1981	1:50	5883	Cell Signaling Technology
AXL Y702	1:50	5724	Cell Signaling Technology
BAD S112	1:200	9291	Cell Signaling Technology
BAD S136	1:50	9295	Cell Signaling Technology
BAD total	1:1000	9292	Cell Signaling Technology
BCL-2 total	1:100	2872	Cell Signaling Technology
BIM total	1:500	2933	Cell Signaling Technology
cABL T735	1:500	2933	Cell Signaling Technology
Caspase 3, cleaved D175	1:50	9661	Cell Signaling Technology
Caspase 9, cleaved D330	1:50	9501	Cell Signaling Technology
cKIT Y703	1:50	3073	Cell Signaling Technology
c-MYC S62	1:100	13748	Cell Signaling Technology
c-MYC total	1:100	9402	Cell Signaling Technology
Collagen Type 1 total	1:50	sc-80760	Santa Cruz
C-RAF S338	1:200	9427	Cell Signaling Technology
Cyclin D1 total	1:100	554180	BD
EGFR total	1:100	2232	Cell Signaling Technology
EGFR Y1068	1:50	2234	Cell Signaling Technology
EGFR Y1173	1:100	44-794	Invitrogen
eIF2alpha S51	1:500	3597	Cell Signaling Technology
eIF4E S209	1:50	9741	Cell Signaling Technology
eIF4G S1108	1:1000	2441	Cell Signaling Technology
ERK1/2 T202/Y204	1:1000	9101	Cell Signaling Technology
ERK1/2 total	1:200	9102	Cell Signaling Technology
Estrogen Rec alpha S118	1:1000	2511	Cell Signaling Technology
Estrogen Rec alpha total	1:50	M7047	DAKO
FGF Rec Y653/Y654	1:1000	3471	Cell Signaling Technology

Fibronectin total	1:50	ab6328	Abcam
FOXM1 T600	1:100	14655	Cell Signaling Technology
FOXO1 S256	1:100	9461	Cell Signaling Technology
FOXO1 T24/FOXO3 T32	1:200	9464	Cell Signaling Technology
GAPDH total	1:100	5174	Cell Signaling Technology
GSK3aB S21/S9	1:100	9331	Cell Signaling Technology
GSK3aB Y279/Y216	1:500	44-604	LifeTechnologies
HER2 total	1:100	2242	Cell Signaling Technology
HER2 Y1248	1:500	IMG-90189	Imgenex
HER2 Y877	1:500	IMG-90185	Imgenex
HER3 total	1:500	4754	Cell Signaling Technology
HER3 Y1197	1:100	4561	Cell Signaling Technology
HER3 Y1289	1:200	4791	Cell Signaling Technology
HSP70 total	1:100	SPA-810	Stressgen
HSP90 total	1:50	4875	Cell Signaling Technology
HSP90a T5/T7	1:100	3488	Cell Signaling Technology
IGF-1 Rec Y1131/Insulin Rec Y1146	1:500	3021	Cell Signaling Technology
IGF-1 Rec Y1135/Y1136_Insulin Rec Y1150/Y1151	1:500	3024	Cell Signaling Technology
IL-6 total	1:100	5143-100	BioVision
Insulin Rec beta total	1:200	3025	Cell Signaling Technology
IRS1 S612	1:200	2386	Cell Signaling Technology
IRS1 total	1:500	2382	Cell Signaling Technology
JAK2 Y1007	1:200	4406	Cell Signaling Technology
Ki67 total	1:100	M7240	Dako/Agilent
LKB1 S334	1:50	3055	Cell Signaling Technology
M-CSF Rec Y723	1:100	3155	Cell Signaling Technology
MEK1/2 S217/S221	1:500	9121	Cell Signaling Technology
MET Y1234/Y1235	1:200	3126	Cell Signaling Technology
MLH1 total	1:500	3515	Cell Signaling Technology
mTOR S2448	1:200	3126	Cell Signaling Technology
NFkB p65 S536	1:100	3031	Cell Signaling Technology
NPM T199	1:100	3541	Cell Signaling Technology
p27 T187	1:200	71-7700	LifeTechnologies
p38 MAPK T180/Y182	1:100	9211	Cell Signaling Technology
p70S6K S371	1:50	9208	Cell Signaling Technology
p70S6K T389	1:100	9205	Cell Signaling Technology
p70S6K T412	1:500	07-018	EMD Millipore
p90RSK S380	1:200	9341	Cell Signaling Technology
p90RSK T359/S363	1:200	9344	Cell Signaling Technology
PARP, cleaved D214	1:100	9541	Cell Signaling Technology
PD-1 total (Nivolumab)	1:100	A2002	Selleckchem

PD-1 total (Pembrolizumab)	1:100	A2005	Selleckchem
PDGF Rec beta Y716	1:200	07-021	EMD Millipore
PDGF Rec beta Y751	1:50	3161	Cell Signaling Technology
PD-L1 total (28-8)	1:500	ab205921	Abcam
PD-L1 total (Atezolizumab)	1:100	A2004	Selleckchem
PD-L1 total (SP142)	1:50	740-4859	Ventana
PI3K p85 Y458_p55 Y199	1:100	4228	Cell Signaling Technology
PRAS40 T246	1:1000	44-1100	Invitrogen
PTEN S380	1:500	9551	Cell Signaling Technology
PTEN total	1:50	9552	Cell Signaling Technology
RB S780	1:2000	3590	Cell Signaling Technology
RET Y905	1:100	3221	Cell Signaling Technology
RON Y1353	1:1000	5176-1	Epitomics
S6RP S240/S244	1:1000	2215	Cell Signaling Technology
SGK1 S78	1:100	5599	Cell Signaling Technology
SRC Family Y416	1:200	2101	Cell Signaling Technology
SRC Y527	1:200	2105	Cell Signaling Technology
STAT1 S727	1:100	9177	Cell Signaling Technology
STAT1 Y701	1:500	9171	Cell Signaling Technology
STAT3 S727	1:100	9134	Cell Signaling Technology
STAT3 Y705	1:100	9145	Cell Signaling Technology
STAT4 Y693	1:100	5267	Cell Signaling Technology
STAT5 Y694	1:50	9351	Cell Signaling Technology
STAT6 Y641	1:100	9361	Cell Signaling Technology
Tuberin/TSC2 Y1571	1:50	3614	Cell Signaling Technology
YAP S127	1:100	13008	Cell Signaling Technology